2008

Discovery and Initial Characterizations of Neurofascin 155 High and Neurofascin 155 Low

Anthony Pomicter
Virginia Commonwealth University

School of Medicine
Virginia Commonwealth University

This is to certify that the thesis prepared by Anthony Dale Pomicter entitled DISCOVERY AND INITIAL CHARACTERIZATIONS OF NEUROFASCIN 155 HIGH AND NEUROFASCIN 155 LOW has been approved by his committee as satisfactory completion of the thesis requirement for the degree of Master of Science

Jeffrey L. Dupree, Ph.D., School of Medicine

Babette Fuss, Ph.D., School of Medicine

Carmen Sato-Bigbee, Ph.D., School of Medicine

John T. Povlishock, Ph.D.

Jerome F. Strauss, III, M.D., Ph.D.

Dr. F. Douglas Boudinot, Dean of the School of Graduate Studies

October 29, 2008

DISCOVERY AND INITIAL CHARACTERIZATIONS OF

NEUROFASCIN 155 HIGH AND NEUROFASCIN 155 LOW

A thesis submitted in partial fulfillment of the requirements for the degree of
Master of Science
at
Virginia Commonwealth University.

by

ANTHONY DALE POMICTER
Bachelor of Science, The Pennsylvania State University, 2002

Director: JEFFREY L. DUPREE
ASSITANT PROFESSOR, ANATOMY AND NEUROBIOLOGY

Virginia Commonwealth University
Richmond, Virginia, United States of America
December 2008

Acknowledgements

I greatly appreciate the patience, guidance, and understanding exhibited by Dr. Jeff Dupree by allowing me to undertake a part-time Master of Science degree while being a full-time employee in his laboratory. His encouragement of my pursuit of higher education made this degree possible. Thank you to Jeff for the experiences, opportunities, and friendship that he has provided to me.

Further support for this degree and directional guidance for the project came from my committee members Dr. Babette Fuss and Dr. Carmen Sato-Bigbee. I appreciate their contributions during committee meetings as well as every time that I had a question regarding "the next step" or what the newest result might mean. Thank you to Babette for her many ideas that came to life through the course of this work. To Carmen I offer enormous appreciation for always making time to discuss my life and my project, my ideas and my struggles.

Dr. John Bigbee, advisor to Dr. Jeff Dupree, has proven to be a mountain of information regarding neuroscience and biochemistry as well as proper navigation of graduate school. I greatly appreciate the time that he took to explain to me all of the things that I suddenly realized I did not understand.

For the kind gifts of antibodies, I am grateful to Dr. Peter Brophy of the University of Edinburgh and Dr. Manzoor A. Bhat of the University of North Carolina. Additionally, Dr. Bhat provided the Caspr KO mice. A special thank you to Dr. Matthew N. Rasband of Baylor College of Medicine for the generous amount of FIGQY antibody; without which this project would not have been possible.

This research was funded by the National Multiple Sclerosis Society and the A.D. Williams Research Award. Microscopy was performed at the Virginia Commonwealth University Department of Anatomy and Neurobiology Microscopy Facility, supported, in part, with funding from NIH-NINDS Center core grant 5P30NS047463.

This document was created in Microsoft Office Word 2003. Images were created in Microsoft Office Publisher 2003 and viewed with Microsoft Office Picture Manager 2003. Images in the "Introduction" taken from publications by other laboratories were viewed and captured with Adobe Acrobat 6.0 Professional.

Table of Contents

Page

List of Abbreviations

Caspr .....contactin-associated protein

CGT.....uridine diphosphate galactose:ceramide galactosyltransferase

CNPs .....2'3'-cyclic nucleotide 3'-phosphodiesterases

CNS.....central nervous system

CST .....cerebroside sulfotransferase

EM.....electron microscopy

ERK2..... extracellular-signal-regulated kinase 2

FIGQY .....phenylalanine, isoleucine, glycine, glutamine, tyrosine-directed antibody

FN3..... fibronectin III-like

Ig .....immunoglobulin

IP .....immunoprecipitation

K^+ .....potassium ion

kDa .....kilo Daltons

KL .....Kaleidoscope ladder

KO..... knockout

MAGs.....myelin-associated glycoproteins

MBPs..... myelin basic proteins

mg..... milli gram, 1×10^{-3} grams

mL ..... milli Liter, 1×10^{-3} Liters

mm ..... milli meter, 1×10^{-3} meters

mM ..... milli molar, 1×10^{-3} molar

MS ..... multiple sclerosis

Na^{+} ..... sodium ion

NAWM ..... normal appearing white matter

ncp1 ..... neurexin IV, Caspr, paranodin 1

Nfasc155 ..... neurofascin 155

Nfasc155H ..... neurofascin 155 high

Nfasc155L ..... neurofascin 155 low

Nfasc186 ..... neurofascin 186

Nfasc140 ..... neurofascin 140

NFC1 ..... neurofascin carboxy terminus one, antibody

N-linked ..... nitrogen-linked

O-linked ..... oxygen-linked

PAGA ..... protein A/G agarose

PAT ..... proline, alanine, threonin-rich

PBS ..... phosphate buffered saline

PLPs ..... proteolipid proteins

PNGase F ..... peptide:N-glycosidase F

PNS ..... peripheral nervous system

PPWM ..... peri-plaque white matter

RIPA ..... radio immunoprecipitation assay buffer

rpm ..... revolutions per minute

SD..... standard deviation

µg ..... micro gram, 1×10^{-6} grams

µL..... micro Liter, 1×10^{-6} Liters

µm ..... micro meter, 1×10^{-6} meters

WT..... wild type

List of Figures

Page

Abstract

DISCOVERY AND INITIAL CHARACTERIZATIONS OF

NEUROFASCIN 155 HIGH AND NEUROFASCIN 155 LOW

By Anthony Dale Pomicter. B.S.

A thesis submitted in partial fulfillment of the requirements for the degree of
Master of Science at Virginia Commonwealth University.

Virginia Commonwealth University, 2008

Major Director: Jeffrey L. Dupree, Ph.D.
Assistant Professor, Anatomy and Neurobiology

This thesis contains the findings from four years of research regarding an oligodendrocyte protein named neurofascin 155. The role of this protein in maintaining adhesion between the myelin sheath of oligodendrocytes and the axons of neurons has become well established in recent years and the research presented here has revealed that while western blots have previously shown one protein/band representing neurofascin 155, there are two proteins/bands. These two proteins have been named neurofascin 155 high and neurofascin 155 low due to their previous inclusion in the single band. The work leading up to their discovery, findings, and the relevance of these two proteins will be discussed in animal models with disrupted myelin:axon adhesion and in the human disease multiple sclerosis.

{CHAPTER 1 Introduction}

"Animal electricity"

Late in the eighteenth century Italian scientist Luigi Galvani inadvertently discovered the role of electricity in life (Piccollini, 2006). The leg of a dead frog was made to twitch and cramp upon addition of a piece of charged metal. Originally termed "animal electricity" and hotly debated as separate from metal-ion based electricity, this discovery led to the invention of the battery by Galvani's colleague and intellectual rival Alessandro Volta. Follow up work has given us the understanding that animal, plant, and all other forms of electricity are the result of the same process; the directed motion of charged particles known as ions.

In animals, the major source of electricity is neurons and the ion responsible for electrical conduction is sodium (Na^+). Named for Latin and Greek terms referring to long, slender objects, neurons are cells that conduct electricity via action potentials to communicate with other cells, sometimes over enormous distances; up to 2.5 meters in the case of giraffes (Badlangana *et al.*, 2007). Neurons in the vertebrate central nervous system (CNS), comprised of the brain, spinal cord, and optic nerves, use electricity to relay the presence or absence of stimulation. The stimulation and ultimate response to it are in the form of chemical signals called neurotransmitters, with some neurons releasing or being receptive to only certain neurotransmitters. For example, the locus coeruleus is the major source of the neurotransmitter norepinephrine in the brain (Foote *et al*., 1983) and while it contains

receptors for many types of excitatory and inhibitory neurotransmitters (Ivanov and Aston-Jones, 1995; Ivanov and Aston-Jones, 2001), it releases only norepinephrine, and the regions that receive input from the locus coeruleus contain norepinephrine receptors (Aston-Jones *et a.l*, 2004).

Neurotransmitters bind the extracellular domain of transmembrane receptor proteins, resulting in the flow of ions, mostly sodium ions (Na^+) and potassium ions (K^+), across the neuronal membrane (Hodgkin and Huxley, 1952; Hille and Catterall, 2006). Binding of the receptor causes, either directly or indirectly, the opening of ion channels and the flux of ions into the neuron. This helps to establish ion gradients across the neuronal membrane. Additionally, other channels contribute to this gradient; sodium:potassium ATPase pumps, for example, consume one molecule of adenosine triphosphate (for energy) to move two Na^+ out of the cell and three K^+ into the neuron (Albers and Siegel, 2006). This inward and outward flow of ions establishes both an electrochemical and concentration gradient, with Na^+ being concentrated outside of the neuron and K^+ inside. The amount of positive charge (Na^+) outside the neuron is in excess of the amount of positive charge (K^+) inside, resulting in a more positive outside; this is called hyperpolarization, basically defined as a "very uneven distribution". This uneven distribution of atoms and charge sets the stage for action potential initiation.

Increased neurotransmitter binding results in increased ion flux and the accumulation of Na^+ inside the neuron. When excess Na^+ accumulates in the neuron and the membrane

polarization is reduced, that is the hyperpolarization is depolarized, resulting in a more even distribution of ions across the membrane, threshold may be reached. Threshold is the point where enough Na^+ has accumulated to activate membrane bound, voltage gated Na^+ channel proteins located at the axon hillock, the transitional region between the neuron cell body and the axon. Intracellular charged amino acids on the channel protein function as voltage sensors and, when a sufficient change in intracellular charge is detected (threshold), cause a conformational change in the protein that results in the opening of the channel. The voltage-gated Na^+ channel is highly specific for Na^+ and since the concentration of Na^+ outside is much greater than the concentration inside, the opening of the channel allows Na^+ to enter the neuron, resulting in the spread of the depolarization. This depolarization spreads to adjacent regions of the axon (upstream Na^+ channels are temporarily inactive), depolarizing them and induces the opening of voltage gated Na^+ channels, and ultimately resulting in the release of neurotransmitter. This spreading depolarization is the action potential (summarized by Hille and Catterall, 2006).

The speed of action potential propagation can be increased in two ways: (1) extremely large caliber axons such as the squid giant axon, which is up to 1 millimeter in diameter, or (2) myelinated neurons (reviewed by Hartline and Colman, 2007). Since size and energy are limiting factors in life, millions of giant axons in one organism has never been observed. Comparisons between a 500 µm unmyelinated squid giant axon and a 12 µm myelinated frog axon show that the unmyelinated axon consumes 5,000 times as much energy and requires 1,500 as much space to conduct at the same speed (Quarles *et al.*,

2006). The savings in space and energy provided by myelin offer an immeasurable evolutionary advantage to an organism, allowing for more fast conducting axons in less space.

Oligodendrocytes and myelin

Insulation by myelin, made by oligodendrocytes in the CNS and Schwann cells in the peripheral nervous system (PNS), prevents the spreading depolarization, termed current, from leaking out of the axon. Myelin is a specialized cell membrane rich in lipids, low in cytoplasm, and typically wrapped around itself numerous times. These wraps increase the distance between the axon's intracellular and extracellular environments. This increased distance decreases the capacitance of the axon's membrane by keeping ions sufficiently separated so that they are no longer attracted to or repelled by each other, allowing them to flow freely upon ion channel activation.

While most cell membranes are half lipid and half protein, myelin is composed of 70-85% lipid and 15-30% protein (Gent *et al*., 1971; Rosetti *et al*., 2008) with spinal cord having a higher ratio of lipid:protein than brain (Quarles *et al*., 2006). The majority of the protein content of myelin is comprised of unique proteins, aiding in the specialized function of myelin as an insulator. Proteolipid proteins (PLPs), for example, comprise ~50% of myelin protein and behave experimentally as lipids due to numerous lipid modifications (Greer *et al.,* 2002). Four isoforms of myelin basic protein (MBPs) comprise ~30% of myelin protein and are unique due to multiple states of phosphorylation and methylation (Quarles

et al., 2006). 2'3'-cyclic nucleotide 3'-phosphodiesterases (CNPs) (Trapp *et al*., 1988) and myelin-associated glycoproteins (MAGs) (Trapp *et al*., 1989) are more minor components of myelin, with each expressed as two alternatively spliced isoforms and often utilized as markers for oligodendrocytes and myelin.

The lipid rich composition of myelin aids in preventing the flow of ions by nature of the lipid bilayer. Lipids can form bilayers as a result of interactions between polar (charged) head groups of adjacent lipids interacting with one another and with water. Also, the non polar (uncharged) tails of lipids are attracted to one another and repel water, facilitating the tail to tail alignment of lipids. These polar and nonpolar interactions enable lipids to pack tightly together, side by side, resulting in bilayer formation. This bilayer structure, as well as interactions with charged proteins (Hu *et al.,* 2004), results in the neutralization of many of the remaining charges in the lipids. Together, the separation of these polar and non polar regions causes the bilayer to have an overall charge of zero. Ions are not attracted to regions of zero charge and will not diffuse through these regions, making lipid bilayers quintessential ion flow barriers and myelin, which is up to 85% lipid, is the highest lipid content membrane known (Nussbaum *et al.*, 1963). By preventing the flow of ions through its own membrane (myelin), the oligodendrocyte increases the resistance of the axon's membrane. Also, myelin is multilamellar, wrapping around the axon numerous times, increasing its effectiveness at decreasing capacitance, increasing resistance, and creating an even larger region of zero charge.

Myelin in the CNS of vertebrates is a distal extension of the cell membrane of oligodendrocytes (translates from Greek as "cells with a few branches") (Figure 1A). Oligodendrocytes can exhibit 40 or more branches (Quarles *et al*. 2006), few compared to the hundreds of branches seen in the dendritic arbors of many types of neurons. Each branch makes contact with an axon, wraps around it many times (Figure 1B), forming a myelin segment. Adjacent myelin segments are separated from each other by nodes of Ranvier (reviewed by Rasband, 2006). The node of Ranvier, commonly referred to as the node, is a specialized axon domain that lacks myelin and contains a high concentration of the voltage gated Na^+ channels responsible for the propagation of action potentials (Chiu, 1980; Waxman and Ritchie 1985; Chiu and Schwarz, 1987). Myelination facilitates the clustering of Na^+ channels at the node so that a single, local depolarizing event can open vast numbers of channels and cause widespread changes in Na^+ concentrations. This concentration change spreads through the long, myelinated region of the axon, due to diffusion and charge repulsion, and activates voltage gated Na^+ channels located further along the axon. Without the clustering of Na^+ channels and insulation created by the myelin sheath, electrical signals are transmitted much slower (Quarles *et al*., 2006) since relatively few channels are activated by a single depolarization and only a small region of the axon is depolarized.

The result of myelination (myelin structure) has been studied for over 50 years (Fernandez-Moran *et al.*, 1950; reviewed by Simons and Trotter, 2007). Many of the characteristics of

Figure 1. Oligodendrocytes are the myelinating cells of the mammalian central nervous system. (A.) An electron micrograph from the laboratory of Dr. Jeff Dupree shows an oligodendrocyte extending process and myelinating several axons in a mouse spinal cord. This oligodendrocyte appears to have myelinated at least seven axons. Numerous small, unmyelinated axons are also shown. (B.) An electron micrograph of a myelinated axon in the rat, adapted from Hiran and Dembitzer, 1967. The individual wraps are myelin are clear at 166,000x and the first (inner) and last (outer) wraps are labeled.

A.

B.

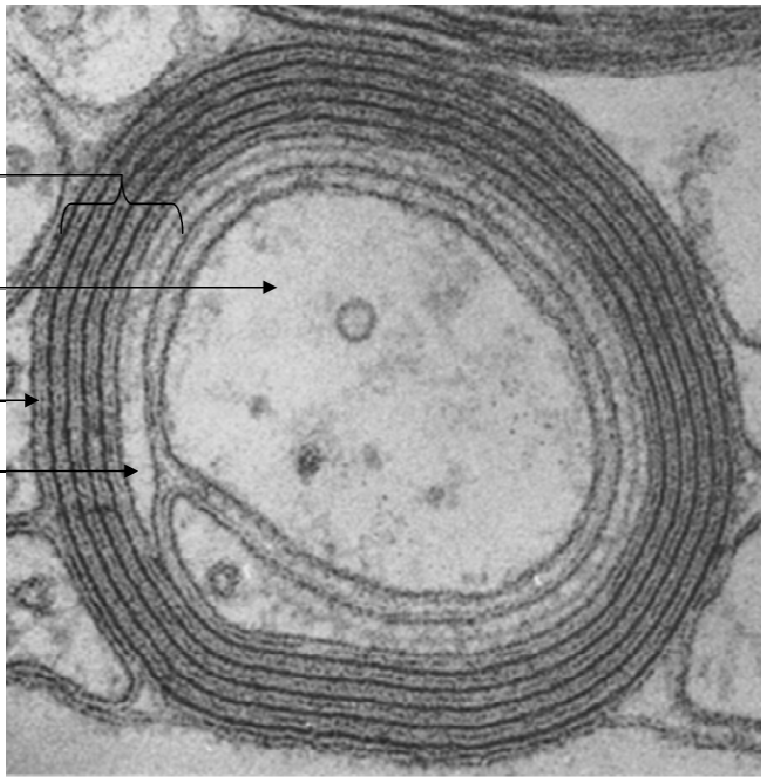

myelin have been thoroughly evaluated in development, disease, and mutant mice (Rosenbluth, 1966; Watanabe *et al*., 1969; Watanabe and Bingle, 1972; Rosenbluth 1976; Kirschner *et al*., 1989; Flores *et al*., 2008) and are beyond the scope of this thesis. Less characterized, but of interest in the last several years are the structural and molecular domains that negotiate the interactions between the myelin sheath and the axon, including, on each side of the node, the paranode, juxtaparanode, and internode (Figure 2A, 2B) (reviewed by Poliak and Peles, 2003). The internode comprises the majority of the length of a myelin segment. In this region the axon and myelin are separated by 12 nanometers (nm) (Peters *et al*., 1976) with myelin:axon adhesion suggested to be mediated by unknown mechanisms involving myelin-associated glycoprotein and myelin galactolipids (Trapp *et al*., 1989; Marcus *et al*., 2002). Internodal myelin is almost completely devoid of cytoplasm, and is therefore called compact myelin. Just nodal to the internode is the juxtaparanode (reviewed by Rasband, 2004). This region lies along the axon and contains concentrations of voltage gated K^+ channels, believed to play a role in re-establishing hyperpolarization following the depolarization that defines action potential propagation. Caspr2 and transient axonal glycoprotein-1, also concentrated at the juxtaparanode, are believed to aid in the stabilization of K^+ channels (Traka *et al*., 2002; Poliak *et al*., 2003; Traka *et al*., 2003).

Regarding the paranode, electron microscopic (EM) analyses suggest that each wrap of myelin is slightly wider than the previous wrap, resulting in successive points of contact between the myelin and the axon (Hirano, 1969). This region of contact is named the

paranode and refers to the regions of myelin and axon on each side of the node. The myelin at the paranode appears as a series of loops when viewed in longitudinal section and are called paranodal or lateral loops. These loops maintain their cytoplasm, giving rise to the name uncompacted myelin. Paranodal loops appear as adjacent rain drop-shaped bulges with one side touching the previous loop, one side touching the subsequent loop, and the bottom "touching" the axon (Figure 2A, 2C). Upon close examination, there is a space of 2-4 nm between the tip of the paranodal loop and the axon such that these two structures are not actually touching (Livingston *et al*., 1973; Dermietzel, 1974). Spanning the gap between the two membranes are structures named transverse bands (Hirano and Dembitzer, 1967) which, in longitudinal EM sections of myelinated axons, appear as small dark slivers. Freeze fracture analysis combined with heavy metal penetration studies revealed that these "bands" form a tube-like structure that completely surrounds the axon (Hirano and Llena, 1995). Transverse bands are believed to play a major role in holding the myelin sheath and the axon together, but their function(s) remain unclear (Rosenbluth *et al*., 2003). Freeze fracture work has shown that while the node and juxtaparanode are molecule rich, presumably corresponding to the Na^+ and K^+ channel proteins, the paranode is relatively molecule poor (Rosenbluth, 1976; Rosenbluth, 1981). Three proteins that cluster at high density in the paranode are neuronal contactin, contactin's trafficking partner contactin-associated protein (Caspr), and oligodendrocytic neurofascin 155 (Einheber *et al*., 1997; Dupree *et al*., 1999; Rios *et al*., 2000; Tait *et al*., 2000).

Figure 2. Nodes, paranodes, and juxtaparanodes are structurally and molecularly distinct domains. (A.) An electron micrograph adapted from Marcus *et al*., 2006 showing the structure of a (rat) CNS myelinated axon in longitudinal section. The node is delineated by arrows and shown in blue, the paranodes in green, and the juxtaparanodes are in red. (B.) An immunolabeled section from a mouse spinal cord demonstrates that sodium channels (Nav1.6, blue), Caspr (green), and potassium channels (Kv1.1, red) are specific to the node, paranode, and juxtaparanode, respectively. Adapted from Zonta *et al*., 2008. (C.) An electron micrograph from Hirano and Dembitzer, 1967 shows transverse bands as dark slivers between the lateral loops of myelin and the axon. The arrow denotes a single transverse band.

A.

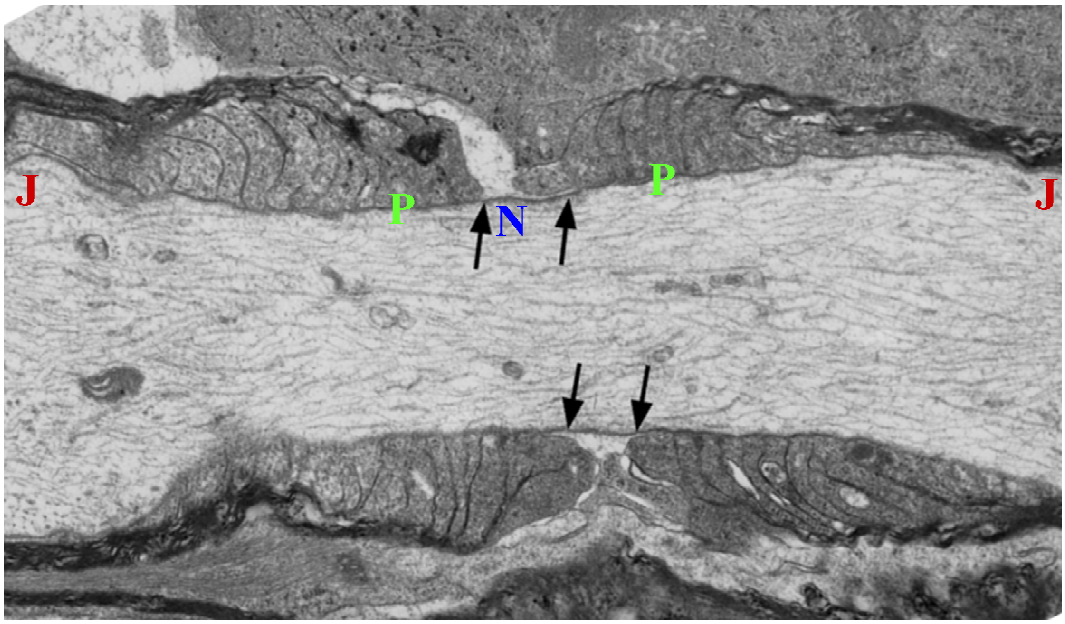

B.

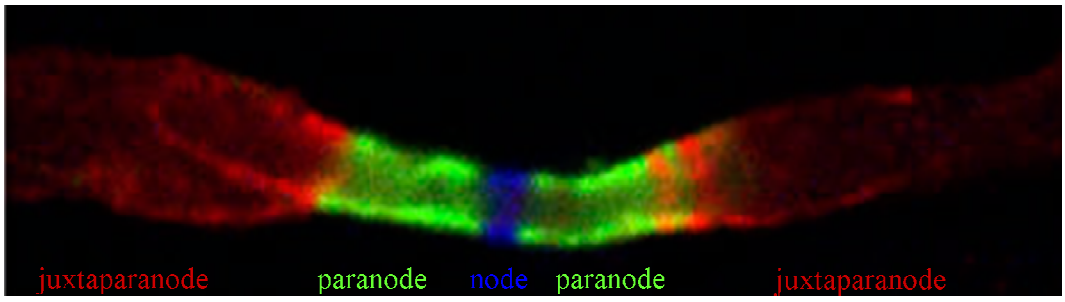

C.

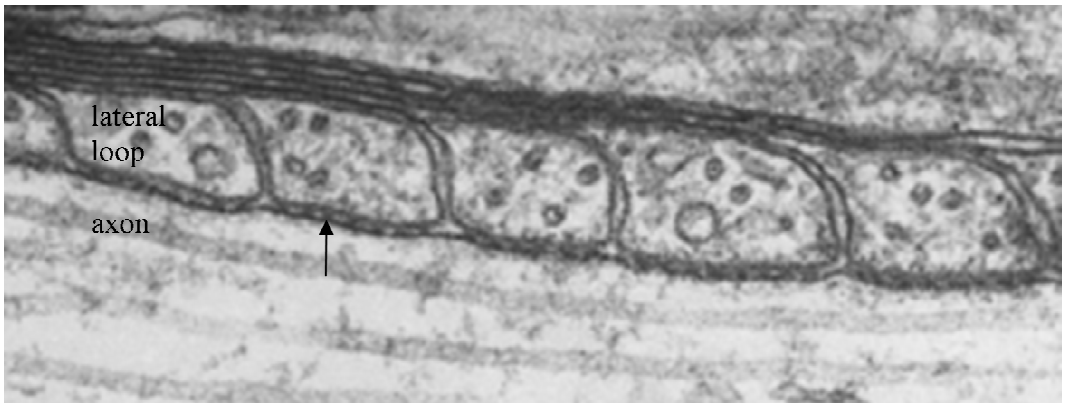

Myelin lipids and sulfatide

The human CNS is over one half lipid (dry weight) (Taylor *et al*., 2004) due to the higher than average lipid content of myelin. Myelin contains concentrations of lipids that are rare in other tissues; galactocerebroside, for example, comprises over 20% of myelin lipid (Coetzee *et al*., 1996a) and over 15% of the total content of myelin but is known to be in only two other tissues, kidney (Costantino-Ceccarini and Morell, 1973; Stahl *et al*., 1994) and colon (Yahi *et al*., 1992), and perhaps pancreas (Buschard *et al*., 1994). The brain contains over 20% of the cholesterol present in the human body and the vast majority of this is in myelin (Dietschy and Turley, 2004). These concentrations of unique and common lipids give the CNS, and more specifically myelin, special properties and provide researchers an interesting environment in which to study the roles of lipids in life. Lipids are used by organisms to store energy in the form of triglycerides, but these types of lipids are nearly absent from the brain (Taylor *et al*. 2004; Gielen *et al*., 2006). Myelin lipids, therefore, must serve other roles. Lipids as structural components are well studied due to their presence in the plasma membranes of all animal cells (Alberts *et al*., 2002) and numerous investigators have recently shown that lipids can also function as signal transducers (reviewed by Hooks and Cummings, 2008 and Pyne *et al*., 2008) and signaling platforms (Zhang *et al*., 2008). While not its only purpose (Menon *et al*., 2003; Boggs *et al*., 2008) it seems that the defining function of myelin is as an insulator and its special lipid composition certainly contributes to this purpose.

Lipids, like proteins, can be modified, including glycosylated (Basu *et al*., 1971), acylated (Lee *et al.,* 2001), phosphorylated (Leevers *et al*., 1996), sulfated (Handa *et al*., 1974), giving rise to tremendous variation in structure and, presumably, function. Recent efforts to tease apart the roles of myelin lipids have used transgenic technology in mice. By removing (knocking out) parts of genes that code for enzymes involved in lipid synthesis, it is possible to create mouse lines that lack a specific enzyme and therefore a specific lipid (or a few lipids). For this purpose, the enzyme uridine diphosphate-galactose:ceramide galactosyltransferse (CGT) was of special interest (Stahl *et al*., 1994; Bosio *et al*., 1996a; Bosio *et al*., 1996b; Coetzee *et al*., 1996a) since its products, galactocerebroside and subsequently sulfatide, both galactolipids, comprise over 25% of the lipid in myelin (Coetzee *et al*., 1996b). Surprisingly, CGT knockout (KO) mice still make myelin, *albeit* less and unstable (Bosio, *et al.*, 1996c; Coetzee *et al*., 1996b). Also of interest, these mice contain abundant glucocerebroside, a lipid that is barely detectable in the normal CNS and suspected of partial functional compensation for the lack of galactocerebroside. Conduction velocity is reduced in spinal cord axons of CGT KO mice in a manner consistent with reduced resistance and/or increased capacitance of the myelin sheath (Coetzee *et al*., 1996b). Additionally, the node and paranode are unstable in the CNS of CGT KO mice and transverse bands do not form (Dupree *et al*., 1998; Dupree *et al*., 1999), suggesting a role for galactolipids in "axo-oligodendrocytic" interactions. Additionally, Coetzee and colleagues (1996b) suggest that galactocerebroside and sulfatide are involved in myelin compaction (removal of cytoplasm) and tight wrapping of the lamellae due to the extensive myelin splitting observed in the ventral column of the spinal cord exclusively in

older (45 day old) CGT KO mice. Adding back the CGT gene to only oligodendrocytes, via the promoter of the proteolipid proteins, resulted in complete recovery of the animal (Zoller *et al*., 2005), suggesting that oligodendrocyte-specific deficits, not neuronal deficits, were responsible for the myelin disruptions.

The formation of compact myelin in the CGT KO mice was surprising and interesting, but did not allow for the functions of galactocerebroside and sulfatide to be distinguished. To pick apart the differing functions of these lipids, another mouse line was created. Honke and colleagues (Honke *et al.,* 2002) generated a mouse that lacks the enzyme cerebroside sulfotransferase (CST), the enzyme responsible for the addition of a sulfate to galactocerebroside to create sulfatide. Sulfatide (Figure 3A) comprises 4-7% of CNS myelin lipid (O'Brien, 1965; Ishazuka, 1997; Gielen *et al*., 2006; Quarles *et al*., 2006). These mice contain normal amounts of CGT mRNA and galactocerebroside but no CST mRNA or sulfatide (Honke *et al*., 2002). Morphological analyses showed that the myelin in these mice is fairly normal up to 15 days of age, with properly compacted but thin sheaths (Marcus *et al*., 2006). Transverse bands were originally not observed in CST KO mice (Honke *et al*., 2002), but do occasionally form (Marcus *et al*., 2006). Although grossly normal in young mice, sulfatide deficient myelin deteriorates with age, showing decreased compaction, increased degenerative sheaths, and nodal and paranodal breakdown (Figure 3B). Accompanying these myelin abnormalities, the CST mice also lose large caliber axons with age. Additionally, it was shown that paired clusters of an oligodendrocyte paranodal protein named neurofascin 155 were lost with age in the

Figure 3. Sulfatide null mice exhibit unstable paranodes. (A.) A schematic representation of the myelin galactolipid sulfatide in its hydroxylated and non-hydroxylated forms, adapted from Avanti Polar Lipids, Inc. The ceramide and galactose-derived components are shown and the sulfate group is circled in red. Mutation of the enzyme cerebroside sulfotransferase (CST KO) prevents the addition of sulfate to the parent molecule galactocerebroside (ceramide plus galactose). (B.) 7 month old CST KO mice and MS patients display everted paranodal loops (arrows and arrow heads), indicating altered interactions between axons and oligodendrocytes. Adapted from Marcus *et al*., 2006 and Suzuki, 1969. (C.) Nfasc155 labeling of the paranode is altered in the CST KO mice at 30 days and 7 months of age. Arrows indicate clusters of labeling, representative of a paranode. In the WT these clusters are typically observed as a pair. 30 day old CST KO mice exhibit increased distance between pairs and more unpaired clusters (arrow heads) while paired clusters are nearly absent from 7 month old CST KO mice. Magnification bar = 10 μm. Adapted from Marcus *et al*., 2006.

A.

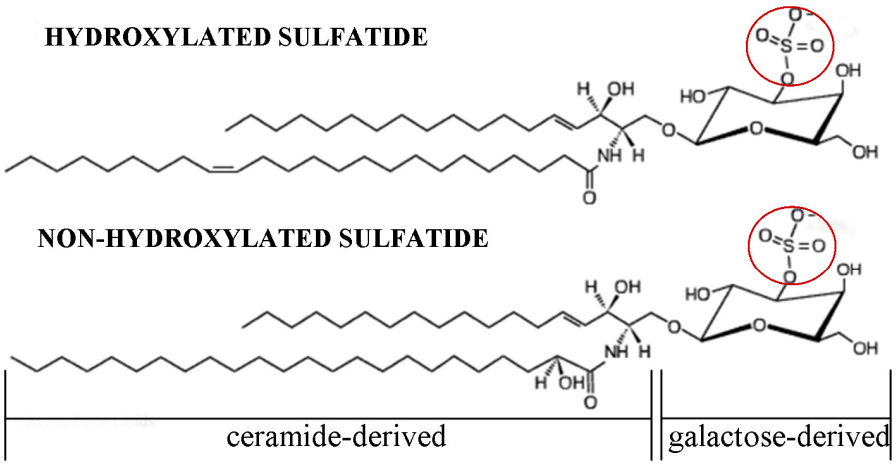

B.

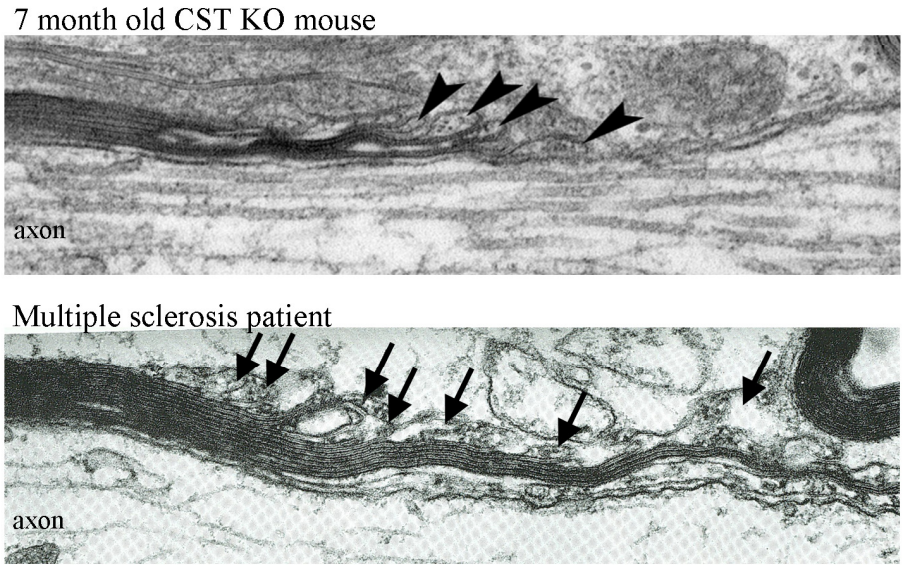

C.

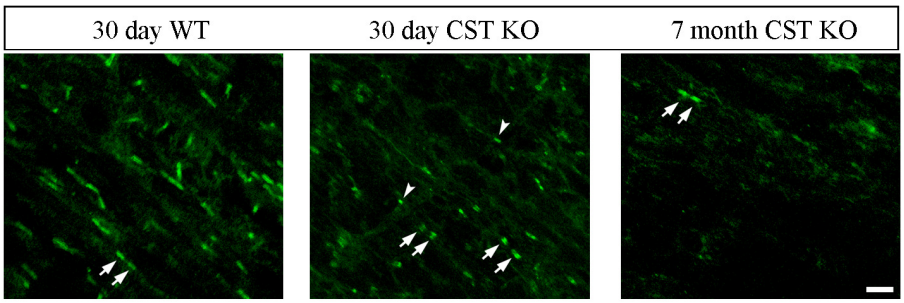

sulfatide null mice (Figure 3C). These investigators concluded that sulfatide is not essential for the establishment of proper myelin or axon structure but is essential for the maintenance of these structures.

Neurofascin 155

Neurofascin 155 (Nfasc155), neurofascin 186 (Nfasc186) and neurofascin 140 (Nfasc140) were originally identified by Rathjen and colleagues in 1987 (Rathjen *et al*., 1987) as proteins of approximately 155, 186, and 140 kilo Daltons (kDa) that bound an antibody directed against glycoproteins from brain plasma membrane extracts. Nfasc140 is a nearly unstudied protein and will not be discussed further in this thesis. Only one protein (Nfasc186) was studied in this first publication and from its apparent function in attaching neurites (fasciculation) to one another in cultures of chicken embryos, the name "neurofascin" arose. Coincidentally, this name is also appropriate for Nfasc155, as it is now believed to play a role in the attachment between the myelin and the axons at the paranode (Tait *et al*., 2000). Interestingly, the chicken neurofascin (Nfasc) gene contains 33 exons and gives rise to at least 50 mRNA transcripts (Hassel *et al*., 1997) but only three proteins are know (Nfasc186, Nfasc155, Nfasc140), indicating extreme alternative splicing and, presumably, functional mRNA. Due to alternative exon usage (Hassel *et al*., 1997) and similarities in amino-terminal sequencing results (Davis *et al.*, 1993), it is believed that these proteins are the result of alternative splicing of the same pre-mRNA and subsequent Southern blots suggest that there is only one Nfasc gene (Collinson *et al*., 1998).

Nfasc proteins are members of the Immunoglobulin (Ig) Superfamily and the L1 subfamily of proteins. Additional members of the L1 subfamily include L1, neuroglial cell adhesion molecule (NgCAM, chicken homologue of mammalian L1), and NgCAM-related cell adhesion molecule (NrCAM), each defined by six Ig-like domains, five fibronectin III-like (FN3) domains, a transmembrane domain, and a highly conserved cytoplasmic domain (Grumet, 1991; Grumet, 1992; Zhao and Hortsch, 1998; Kenwrick *et al*., 2000). Structural analyses of Nfasc186 and Nfasc155 revealed subtle differences in their amino acid sequences (Figure 4A) (Volkmer *et al.*, 1992). The Nfasc gene contains exons encoding the following major protein domains: (Amino-terminus) signal sequence, six Ig-like domains (C2 class), four FN3 domains, a mucin-like/PAT (proline, alanine, threonine rich) domain, a fifth fibronectin III-like domain, a transmembrane domain, and a cytoplasmic domain (Carboxy-terminus). An early publication stated that there were four FN3 domains (Volkmer *et al.*, 1992), but the same laboratory later discovered that there are two exons encoding a fifth FN3 domain located between the mucin-like and transmembrane domain-encoding exons in both chicken and rat Nfasc (Hassel *et al*., 1997). This fifth FN3 domain has been observed in the gene and in several cDNAs but its presence in Nfasc proteins has not been evaluated and it is assumed by some investigators to be absent from Nfasc proteins (Tait *et al*., 2000) while others assume that it is present in Nfasc186 (Koticha *et al*., 2005). The third of these FN3 domains is exclusive to Nfasc155 while only Nfasc186 contains the mucin-like/PAT domain. Other identifying sequence components that differentiate Nfasc155 from Nfasc186 include: N-terminal SIGQNE minor domain (Nfasc186 only), 17 amino acid insertion domain between Ig-like domains 2 and 3

Figure 4. Nfasc155 is an adhesion protein concentrated at the myelin paranode. (A.) A schematic presenting the similarities and differences between oligodendrocytic Nfasc155 and neuronal Nfasc186. The ? represents the unevaluated fifth fibronectinIII-like domain. Adapted from Davis *et al*., 1996. (B.) Nfasc155, contactin, and Caspr concentrate at the paranode and not the node, juxtaparanode, or internode. Sodium channels (NaCh) concentrate at the node and potassium channels (KCh) concentrate at the juxtaparanode. Yellow indicates green and red labeling in the same plane. Adapted from Sherman *et al*., 2005 and Howell *et al*., 2006. (C.) Nfasc155 and Caspr localize to the mesaxon, the spiraling point of contact between the first wrap of myelin and the axon (arrow). Adapted from Tait *et al.,* 2000.

A.

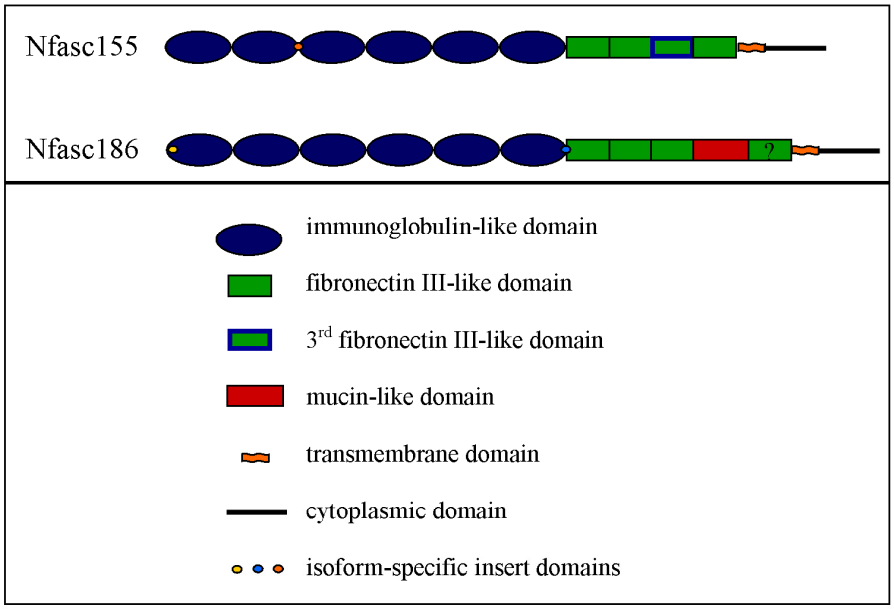

B.

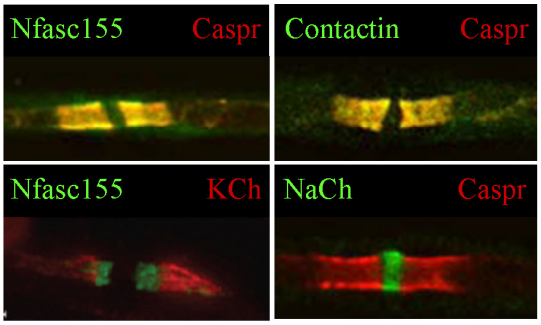

C.

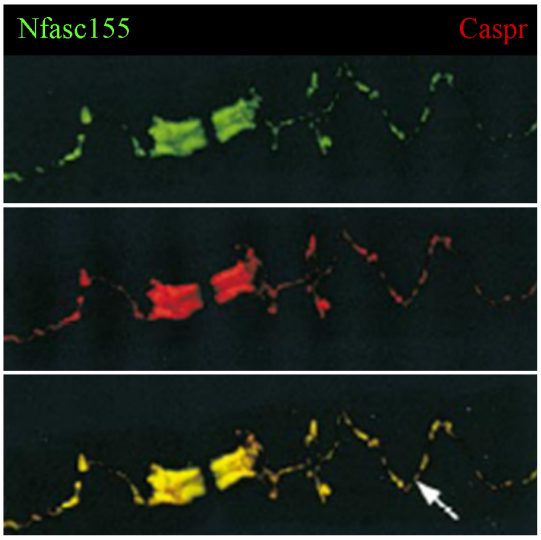

(Nfasc155 only), and 15 amino acid insertion domain between Ig-like domain 6 and FN3 domain 1 (Nfasc186 only) (Davis *et al.*, 1996). Interestingly, it is known that the Nfasc155-specific third FN3 domain is difficult to make specific antibodies against (Davis *et al.,* 1996) and the same observation has been personally communicated by Dr. Manzoor Bhat, University of North Carolina. Ig domains are the defining characteristic of antibodies due to their role in protein:protein interactions (reviewed by Barclay, 2003) while the FN3 domains are so named due to their homology to the type III module of the macromolecule-binding glycoprotein fibronectin (Chernousov *et al*., 1991; Davis *et al*., 1993). Similarities to Ig and FN3 domains define the L1 subfamily and imply that neurofascin proteins have protein binding capabilities.

The mucin-like/PAT domain of Nfasc186 is predicted to be rich in sites of O-linked (oxygen-linked) glycosylation (Volkmer *et al*., 1992) and O-sialoglycoprotease (O-sialoglycoprotein endopeptidase) degrades Nfasc186 but not Nfasc155 (Davis *et al*., 1996), indicating that Nfasc155 does not contain O-linked glycosylation. Lectin binding studies in conjunction with enzymes that specifically remove N-linked (nitrogen-linked) glycosylation (peptide:N-glycosidase F (PNGase F) and endoglycosidase H have been used to determine that both proteins contain N-linked carbohydrates, but that not all predicted sites are glycosylated (Davis *et al*., 1996). The transmembrane domain of Nfasc186 can be palmitoylated *in vitro* (Ren and Bennett, 1998), suggesting membrane microdomain (lipid raft) incorporation *in vivo,* and while the transmembrane domains of Nfasc186 and Nfasc155 are 100% conserved, palmitoylation of Nfasc155 has not been

evaluated. The membrane microdomain incorporation of Nfasc155 has been tested, however, and it is considered to be a lipid-raft protein by the definitions set forth by the authors (Schafer *et al*., 2004).

The proposed function of Nfasc155 as an adhesion molecule negotiating the attachment of the myelin sheath to the axon is strengthened not only by its make up of protein binding domains but also by its apparent colocalization (Tait *et al*., 2000) with contactin (Ranscht *et al*., 1984) and contactin-associated protein {Caspr (Peles *et al*., 1997), also known as paranodin (Menegoz *et al*., 1997) and ncp1 (neurexin IV, Caspr, paranodin 1, Bhat *et al*., 2001)}, both of which are also concentrated at the neuronal paranode, (Einheber *et al*., 1997; Rios *et al*., 2000) (Figure 4B). While the exact details of their interaction is still debated (Bonnon *et al*., 2003; Gollan *et al*., 2003), it seems that contactin and Caspr associate in the endoplasmic reticulum of the neurons and that contactin is required for the proper trafficking of Caspr to the paranode (Peles *et al*., 1997; Bonnon *et al*., 2003). N-linked glycosylation states of contactin play a role in binding to Caspr as well as in its localization to the paranode (Bonnon *et al*., 2003; Gollan *et al*., 2003) and contactin exists as two glycoforms (high and low molecular weight contactin) in rat brain, one sensitive and one resistant to endoglycosidase H while both are sensitive to PNGase F, indicating differing complexities of carbohydrates for each glycoform. Once localized, contactin, also a member of the Ig Superfamily, is held in the membrane by glycosylphosphatidylinositol linkage and perhaps through its binding with Caspr (anchored via a transmembrane domain, Poliak and Peles, 2003). Contactin has been shown to bind Nfasc155 both with

(Charles *et al*., 2002) and without (Gollan *et al*., 2003) Caspr. Due to the concentration of these proteins at the paranode and mesaxon (the spiraling point of contact between the myelin sheath and the axon, Figure 4C), their abilities to interact, and the overall lack of particles in this region, this trimolecular complex is believed to be a major component of transverse bands. Additionally, mice deficient in either contactin (Boyle *et al.,* 2001), Caspr (Bhat *et al*., 2001) or the gene for neurofascin (missing all neurofascin proteins, Sherman *et al*., 2005; Zonta *et al*., 2008), lack transverse bands. Recently, Nfasc186 was reintroduced into the neurofascin KO mouse, creating a Nfasc155 KO mouse (Zonta et al., 2008). In this mouse, contactin and Caspr do not localize to the paranode while the nodal architecture is molecularly restored.

Multiple sclerosis

Multiple sclerosis (MS), the most common demyelinating disease of the human CNS, is defined by focal loss of myelin, termed plaques (reviewed by Trapp *et al*., 1999). One of the goals of MS research is to understand the initial events that take place in the disease, thus suggesting a cause. Plaques occur in myelin-rich (white matter) regions of the CNS and are often studied to obtain information regarding whether the myelin or the oligodendrocyte received the initial insult and how damage occurred (Black *et al*., 2007; Han *et al*., 2008). In addition, the regions near plaques, normal appearing white matter (NAWM) and peri-plaque white matter (PPWM), are also studied since these regions have existed in the same environment as the now afflicted area, but lack gross demyelination (Zeis *et al*., 2008). Recently, subtle paranodal abnormalities have been observed in PPWM

as well as at the plaque edge and center, including elongation of the paranode (visualized with anti-Nfasc155 and anti-Caspr) and abnormal localizations of juxtaparanodal K^+ channels and Nfasc155, in the presence of a molecularly normal node (Wolswijk and Balesar, 2003; Howell *et al.,* 2006). These paranode-specific alterations are consistent with disruptions at the paranode preceding demyelination and axonal pathology in MS.

Questions remain regarding the formation and stability of the paranode

Three transmembrane proteins located at the paranode, contactin, Caspr, and Nfasc155, are able to bind to each other in ways that are still unclear and controversial. Results are inconclusive as to whether the high or low molecular weight glycoform of contactin is responsible for the binding of Nfasc155 while Caspr has been shown to aid (Charles *et al*., 2002; Bonnon *et al*., 2003) and inhibit (Gollan *et al*., 2003) contactin:Nfasc155 binding. Absence of Nfasc155 results in the absence of contactin and Caspr from the paranode (Sherman *et al*., 2005; Zonta *et al*., 2008), while Nfasc155 has been shown to aid in orchestrating proper molecular arrangement of the node (Zonta *et al*., 2008), suggesting that Nfasc155 plays a major role in the assembly of both the node and paranode. The absence of myelin galactolipids in the CGT (Bosio *et al*., 1996; Coetzee *et al*., 1996) and CST KO (Honke *et al*., 2002; Marcus *et al*., 2006) mice, for unknown reasons, show paranodal phenotypes similar to contactin, Caspr, and Nfasc KO mice. The results presented in this thesis suggest answers to some of these questions.

{CHAPTER 2 Materials and Methods}

Mice

Mice heterozygous for the cerebroside sulfotransferase (CST) gene were obtained from Dr. Koichi Honke (Honke *et al*., 2002). Breeding of these mice results in Mendelian distributions of wild type (WT, +/+), heterozygote (+/-), and CST knockout (CST KO, -/-) individuals. CST Forward, Long and CST Reverse, Long primers were utilized for genotyping the CST mice: (CSTFL: 5'-CTA TTG GAC AAC TAC CCA CTA CCA CCT GC-3' and CSTRL: 5'-GCA CTT ATG TCC GTG TGA GAG TGT CAG GTC-3'). The neo cassette (only present in the mutated CST gene) was amplified with the primers CST Neo cassette forward and CST Neo cassette reverse: (CSTNEOF: 5'-CAT TCG ACC ACC AAG CGA AAC ATC G-3' and CSTNEOR: 5'-GCA CGA GGA AGC GGT CAG CCC AAT-3'). PCR cycles were as follows: 95°C for 5 minutes, [95°C for 10 seconds, 60°C for 10 seconds, 68°C for 20 seconds] for a total of 30 cycles with Sigma-Aldrich's Klentaq DV Ready Mix (St. Louis, MO). WT mice yield only one band at 548 bases, KO mice yield one band at 332 bases, and heterozygous mice yield both sizes. Mice were bred and maintained in an AAALAC certified facility and all protocols were approved by the Institutional Animal Care and Use Committee of Virginia Commonwealth University.

Mice mutated at the contactin-associated protein (Caspr) locus were obtained from Dr. Manzoor Bhat at the University of North Carolina (Bhat *et al.,* 2001). Survival beyond post natal day 21 is rare; accordingly, tissue was harvested at the oldest age available (day 19).

Protein preparation

Mice were deeply anestatized with 2.5% 2,2,2 tribromoethanol (known as Avertin, Sigma-Aldrich) in 0.9% NaCl at 0.016 milli Liter (mL) per gram of body mass and decapitated. Whole brains and spinal cords were rapidly removed, placed separately in a microcentrifuge tube, placed in liquid nitrogen then -80°C for long term storage. Samples were drill homogenized on ice in either phosphate buffered saline (PBS: 137 millimolar (mM) NaCl, 10 mM Na_2HPO_4, 1.8 mM KH_2PO4, 2.7 mM KCl, pH 7.4) or radioimmunoprecipitation assay buffer (RIPA: PBS with 0.1% sodium dodecyl sulfate (Fisher, Thermo-Fisher, Pittsburgh, PA), 0.5% sodium deoxycholate (Sigma-Aldrich), 0.1% nonidet P-40 (Pierce, Thermo-Fisher, Rockford, IL) containing protease inhibitor cocktail (Sigma-Aldrich) for 3 minutes, (2-3 mL, spinal cord) or 5 minutes (5 mL, brain) at 4000 revolutions per minute (rpm). Homogenates were centrifuged in a microcentrifuge for one minute at 13,000 revolutions per minute to remove remaining pieces of tissue and insoluble material. The supernatant was removed to a new tube; a 50 µL sample was set aside for protein assay, and stocks were stored at -20°C until protein assay was completed. Protein concentrations were determined with the Micro BCA Protein Assay Kit by Pierce according to the manufacturer's protocol. Dilutions of bovine serum albumin were used to create the standard curve. Four dilutions per sample, triplicate of each, were made and

compared to the standard curve (absorbance at 562 nanometers) using the Spectra Max Plus spectrophotometer (Molecular Devices, Sunnyvale, CA). Protein concentrations were determined for each dilution, averaged, and one half of each sample was diluted to two µg per µL with RIPA. To this, one volume of final sample buffer (Laemmli, 1970), now known as Laemmli sample buffer (Bio-Rad, Hercules, CA: 62.5 millimolar Tris-HCl, pH 6.8, 2% sodium dodecyl sulfate, 25% glycerol, 0.01% Bromophenol Blue), containing 5% freshly added β-mercaptoethanol (Sigma-Aldrich) was added and samples were aliquoted at 100 µL per tube and stored at -80°C. Prior to loading onto a gel, protein samples were incubated in a 100°C heat block for 5 minutes, briefly centrifuged to collect all fluid, mixed with a pipet tip and added to the gel.

Western blotting

For gel electrophoresis, 20-25 µg of spinal cord proteins and 40-50 µg of brain proteins were run on 10% Ready Gels (Bio-Rad) containing 10 wells with a maximum volume of 50 µL per well. Gels were run in electrode buffer (192 mM glycine, 25 mM Tris, 0.1% sodium dodecyl sulfate) with Bio-Rad's Mini Protean 3 cell and power was supplied by Bio-Rad's Power Pac HC. For repeatable separation of neurofascin 155 high and neurofascin 155 low, the gels were run until the 75 kDa band of the Kaleidoscope ladder (Bio-Rad) was at the bottom of the gel (approximately 30 minutes at 70 volts then 2 hours at 150 volts). Upon completion of the run, gels were carefully removed from their holding apparatus and misshapen edges were removed while the lanes and stacking gel were cut off the top.

The gel was soaked in transfer buffer (192 mM glycine, 25 mM Tris with 20% methanol, stored at -20°C while the gel was running) for 10-20 minutes. The gel was prepared for transfer as follows: negative (black) side of the clamp down, absorbent mesh, Mini Trans Blot Filter Paper, gel (left front of the gel facing down and right), 0.45 µm pore size nitrocellulose (roll out bubbles), Mini Trans Blot Filter Paper (roll out bubbles), absorbent mesh. The clamp was carefully shut and placed in the transfer apparatus along with a small stir bar. The apparatus was placed in an ice-water bath approximately five times the volume of the apparatus and the bath plus apparatus was placed on a magnetic stirrer set to low spin throughout the transfer. The proteins were transferred for two hours at 100 volts, with an internal ice change after one hour. Upon completion of the transfer, the sandwich was disassembled and the membrane immediately placed in excess PBS and placed on a rotator. PBS was changed every ten minutes for a total of three changes and the membrane was blocked in 5% non-fat dry milk (Bio-Rad) in PBS containing 0.05% Tween-20 (Sigma-Aldrich) for 45 minutes. Primary antibodies were incubated at 4°C overnight on a rotator; FIGQY at 1:2,000, NFC1 at 1:40,000. ERK2 dilutions varied depending on the amount and origin of the protein loaded; 1:1000 for under 10 µg, 1:5,000 for 10-20 µg, and 1:10,000 for over 20 µg of spinal cord protein and 1:50,000 for 40 µg of brain protein. The following day, the antibody was removed and the membrane was rinsed several times in PBS until milk was no longer visible. The membrane was incubated in PBS with changes every ten minutes for a total of three changes then blocked a second time for 30 minutes in 5% milk PBS containing 0.05% Tween-20. Secondary antibodies conjugated to horse radish peroxidase (Santa Cruz Biotechnology, Santa Cruz, CA) were diluted 1:10,000

(added to the block) and incubated with the membrane for two hours at room temperature (20-25°C). Following the removal of the secondary antibody, PBS was added and changed until milk was no longer visible, and PBS containing 0.05% Tween-20 added for 10 minutes with one change. Finally, the membrane was rinsed three times with PBS, ten minutes each time. SuperSignal West Dura Extended Duration Substrate (Pierce) allowed for visualization of the locations of the proteins of interest. Imaging and image analysis performed with the AlphaInnotech Fluorchem SP device and AlphaInnotech AlphaEase software (San Leandro, California).

Immunohistochemistry

A 7 day old rat pup was anesthetized with avertin (2,2,2, tribromoethanol, 2.5% (w/v) in 0.9% sodium chloride) and transcardially perfused with 4% paraformaldehyde (pH 7.3). The spinal cord and brain were immediately harvested, cryopreserved in 30% sucrose in PBS, frozen in Optimal Cutting Temperature compound (Sakurak, Torrance, CA), and sectioned at 10 µm. Sections were double immunolabeled with antibodies directed again neurofascin proteins (named FIGQY) and Caspr. Briefly, sections were incubated in -20°C acetone for 10 minutes, blocked in PBS containing 10% cold water fish gelatin and 0.1% Triton X-100. Primary antibodies were diluted in the blocking buffer at 1:200 (FIGQY) and 1:1000 (anti-Caspr), incubated overnight at 4°C, and sections were washed in PBS and blocked a second time. Appropriate fluorescent labeled secondary antibodies were incubated with the sections for 90 minutes and visualized with a Leica TCS-SP2 AOBS laser confocal microscope. Images were collected a maximum projection Z stack images

compiled from six optical sections using a 63x oil immersion objective with a numerical aperature 1.3. Microscopy was performed at the Virginia Commonwealth University Department of Anatomy and Neurobiology Microscopy Facility.

Antibodies, loading control, and molecular mass standards

The rabbit polyclonal pan-neurofascin antibody known as "FIGQY" is named after the amino acid sequence phenylalanine, isoleucine, glycine, glutamine, tyrosine located in the C-terminal antigen CSFIGQYTVRK (Ogawa *et al*., 2006). This antibody was generated in the laboratory of Dr. Matthew Rasband, Baylor College of Medicine, and I greatly appreciate his generosity in providing the ample amounts of antibody required for this project. The FIGQY region was chosen because the tyrosine residue has been previously shown to play a role in phosphorylation-state dependent cytoskeletal interactions (Tuvia *et al*., 1997) and Dr. Rasband personally communicated that the FIGQY antibody was generated to be phosphorylation-state specific, but it is not. A second rabbit polyclonal pan-neurofascin antibody known as "NFC1" and directed against the extreme C-terminus sequence CGNESSEATSPVNAAIYSLA was obtained from Dr. Peter Brophy, University of Edinburgh (Tait *et al*., 2000). Both FIGQY and NFC1 are directed against the cytoplasmic, C-terminus region of neurofascin proteins but the two antigen sequences do not overlap.

To control for loading of the gel and transfer of the proteins from the gel to the nitrocellulose, extracellular-signal-related kinase 2 (ERK2) was detected with a rabbit

polyclonal IgG antibody (clone C14, Santa Cruz Biotechnology). This protein fits all of the parameters for a potential loading control: (1) present during the time point(s) of interest (2) unaltered levels during the time point(s)/treatments of interest (3) readily detectable with an available antibody (4) molecular mass fits into the project.

The apparent molecular masses of proteins were estimated on the membrane with Magic Mark XP Western Standard (MM) (Invitrogen, Carlsbad, California), a standard detected by various HRP-conjugated secondary antibodies. Kaleidoscope Ladder (KL) (Bio-Rad) allows for monitoring of a gel run and the efficiency of transfer. Eight µL of this ladder is completely transferred during a two hour electrophoretic transfer at 100 volts. The red, 75 kDa band was run to the bottom of the gels to allow for optimal separation of the proteins examined.

PNGase F

Peptide: N-glycosidase F (PNGase F, New England Biolabs, Ipswich, MA) is an enzyme that removes N-linked carbohydrates from proteins. The enzyme cleaves between the asparagine containing the carbohydrate and the first N-acetylglucosamine, removing the entire carbohydrate and leaving an aspartic acid residue in place of the asparagine. For establishment of the protocol and deglycosylation for western blot experiments, 20-70 µg of protein was denatured in 1x glycoprotein denaturing buffer (10x is 5% sodium dodecyl sulfate, 0.4 molar dithiothreitol) at 100°C for ten minutes and deglycosylated by incubating with 1x G7 reaction buffer (10x is 0.5 molar sodium phosphate, pH 7.5), 1% nonidet P-40,

and 1-3 µL PNGase F at 37°C for one-four hours. For experiments designed to deglycosylate abundant immunoprecipitated proteins of interest, approximately 400 µL of purified, denatured glycoprotein in 1x glycoprotein denaturing buffer was brought to 700 µL with 1x G7 reaction buffer, 1% nonidet P-40, water, 5 µL PNGase F and incubated at 37°C for two hours. One volume of Laemmli sample buffer containing 5% β-mercaptoethanol was added to stop the reaction and the samples were stored at -20°C.

The NetNGlyc Server 1.0 (http://www.cbs.dtu.dk/services/NetNGlyc/) was used to predict locations of N-linked glycosylation (PubMed accession AAL27854, rat Nfasc155 kDa isoform) as well as the likelihood that a given site is glycosylated *in vivo*. Highly likely is defined as above 0.5 threshold, 9/9 neural networks agreeing on the outcome, and a + + result. Somewhat likely is defined as above 0.5 threshold, 6 or more neural networks agreeing on the outcome, and a + result. Only NXS/T (asparagine, any amino acid, serine or threonine) sequons free of proline and located in the cytoplasmic region were considered. Molecular mass was calculated with the ExPASy Compute pI/MW tool available at www.expasy.ch/tools/pi_tool.html.

Human tissue

Brain and spinal cord tissues were obtained upon request from Rocky Mountain Multiple Sclerosis Center (www.mscenter.org; Englewood, CO). Three main categories of brain tissues were received: non multiple sclerosis (MS), normal appearing white matter (NAWM) from MS patients, and MS patient tissue. For spinal cords, only MS patient

tissue was available. Four of each, non MS and NAWM, eight MS brain samples, and six spinal cord samples were received. Samples were approximately six by three centimeters. One-third of each sample was cut off, homogenized in one mL RIPA buffer and processed for western blot as stated above.

Immunoprecipitation

In an attempt to identify the proteins of interest with mass spectrometry, optimal conditions for the immunoprecipitation (IP) of neurofascin 155 high and neurofascin 155 low were determined empirically as follows. Mouse spinal cord homogenates in RIPA alone showed very little protein of interest following IP with the FIGQY antibody. Pretreatment of the homogenates with 1% Triton X-100 (ICN Biomedicals, Inc., Aurora, OH) resulted in a dramatic increase in the amount of protein recovered; perhaps due to the disruption of lipid spheres containing neurofascin proteins (via its hydrophobic, transmembrane domain) where the cytoplasmic antigen sequence would be inaccessible to the antibody/antibodies. All centrifugation steps in the IP are 5,000 rpm for one minute, however, since the pellet is the point of interest, all homogenates were pre-centrifuged for five minutes at 13,000 rpm the day that they were homogenized and one minute at 8,000 rpm the day of the IP to remove insoluble material. To remove endogenous antibodies and other naturally adhesive molecules, homogenates were treated with Protein A/Protein G agarose plus (PAGA, Santa Cruz Biotechnologies) for two hours in a 4°C cold room on an inverting rotator. Samples were centrifuged, the pellet discarded, and the supernatant incubated with FIGQY primary antibody. Incubations and volumes varied depending on

whether the purpose was to work out the basic protocol or to capture enough protein for downstream use. To work out the basic protocol, 500 µg of spinal cord protein and 10 µL of FIGQY primary antibody yielded enough protein of interest to be visualized by western blot. To attempt to identify proteins by mass spectrometry and consume a minimum of antibody, serial IP was conceived. Serial IP is the repeated IP of one supernatant to evaluate the volume of antibody required to remove all target protein from the supernatant. It was found that approximately 100 µL of FIGQY can remove virtually 100% of the proteins of interest from one adult rat spinal cord homogenate (roughly 45 mg of protein). Since this method worked with "only" 100 µL of FIGQY and other methods consumed more yet yielded less than 100% target, the serial IP method was utilized further. One half of one adult rat spinal cord homogenate was incubated with 200 µL PAGA for two hours (all steps are at 4°C on an inverting rotator), centrifuged to remove the PAGA and any endogenous matter that it bound, and the supernatant was incubated with 50 µL of FIGQY for 2-4 hours then 100 µL of PAGA overnight. The following day, the IP was centrifuged, the pellet washed twice with cold RIPA and stored on ice while the supernatant was incubated with 20 µL of FIGQY for two hours followed by 50 µL of PAGA for two hours. This step was repeated, consuming 90 µL of FIGQY total and yielding a pellet of PAGA and target of approximately 100 µL. The second half of the rat spinal cord was then treated with Triton X-100 and 200 µL of PAGA and incubated overnight with the PAGA:target pellet and another 10 µL of FIGQY. The following day, the pellet was washed four times with cold RIPA and proteins eluted in 300 µL 1x glycoprotein denaturing buffer (from the PNGase F protocol) at 100°C for ten minutes, centrifuged, supernatant harvested, and

another 100 µL 1x glycoprotein denaturing buffer added to the pellet, heated, centrifuged, harvested. Eluted proteins (~450 µL) were treated with 5 µL of PNGase F (see PNGase F, Materials and Methods). Deglycosylated samples were centrifuged in centricon-30 columns (Centricon, now Millipore, Billerica, MA) for one to two hours at 6,000 rpm at 4°C to reduce the volume sufficiently for gel electrophoresis. The centrifugation was monitored periodically and stopped when the fluid reached 40 µL. Following the protocol provided with the columns, the tubes were inverted, placed in a collection vial, and centrifuged at 2,000 rpm for five minutes to collect the protein concentrate. Laemmli sample buffer was added (40µL) and 50 µL was loaded on a gel.

{CHAPTER 3 Results}

Neurofascin 155 is reduced in sulfatide null mice

In 2006, this laboratory published that Nfasc155 clusters in the paranode of sulfatide null mice but, unlike WT littermates, these clusters deteriorate with age, resulting in nearly complete loss of paranodal clusters by 7 months of age (Marcus *et al*., 2006). The current project began as an inquiry into whether this dramatic loss of paranodal clustering of Nfasc155 was due to reduced clustering of Nfasc155 at the paranode or loss of Nfasc155 altogether. As shown in Figure 5A, spinal cord homogenates from 15 day, 30 day, and 7 month old CST KO mice contain less Nfasc155 than their respective littermate WT. Fifteen day old sulfatide null spinal cords contain 52% less Nfasc155 (standard deviation (SD)=33%, p=0.003) than littermate WT (SD=21%). By 30 days of age, Nfasc155 is 24% reduced (SD= 14%, p=0.044) in the CST KO compared to WT (SD=16%). While the 7 month old CST KO mice appear to contain 40-60% less Nfasc155, attempts to quantify these results yielded numbers that did not always match what the western blot suggested and this will be addressed in the next section. Figure 5B shows that both the 46 and 48 kDa isoforms of CNP follow their normal expression profiles and that the abundance of each isoform is unaltered by the absence of sulfatide at 15 days, 30 days, and 7 months of age. Unpublished work from this laboratory shows that CNPs are expressed normally at birth, 3 and 7 days of age in the CST KO and that MBPs levels are unaltered at all ages mentioned (data not shown). Together, these results suggest that myelin proteins are expressed normally and that Nfasc155 is present, *albeit* at reduced levels, in the absence of sulfatide,

Figure 5. Nfasc155 is significantly and specifically reduced in the absence of sulfatide. (A.) Western blot analysis of Nfasc155 shows significant decreases at 15 (52%) and 30 days (24%) of age. While Nfasc155 appears reduced in the 7 month old CST KO, this was not significant, believed to be due to observed inconsistencies between the WT and CST KO. Evaluation of these inconsistencies led to the results shown in Figure 5. Nfasc140 is visible just below Nfasc155 in the 7 month old WT. (B.) CNP 48 (CNP high) levels are not altered in the absence of sulfatide and the CNP 46 (CNP low) expression profile is also normal. Additionally, MBP levels are normal in the CST KO mice at these same ages (unpublished observations from this laboratory), demonstrating a specific reduction in Nfasc155 in the absence of sulfatide.

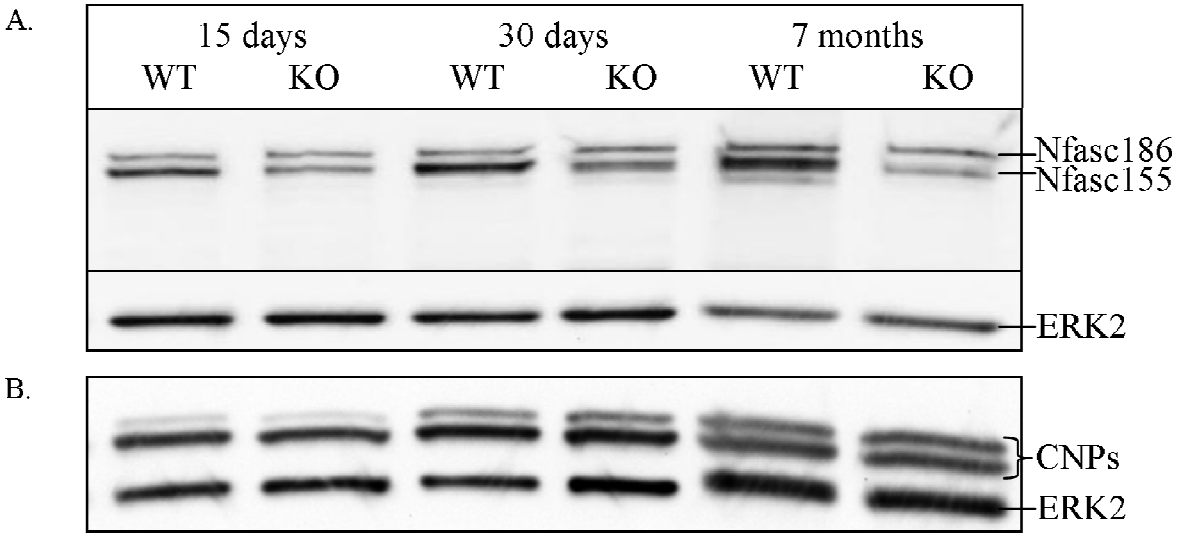

indicating that the near complete loss of paranodal clusters at 7 months of age is due to reduced clustering, not a loss of the protein itself.

The neurofascin 155 band seen on western blots contains two bands, one of which is altered in the absence of sulfatide

The process of optimizing the separation of Nfasc186 and Nfasc155 showed irregular results, especially in animals 3 months of age and older. Most notably, there appeared to be a shift in the location of Nfasc155, without a comparable shift in Nfasc 186, in the CST KO, leading to experiments designed to address this issue. Further optimization resulted in gel runs in excess of two hours and it was realized that WT mice three months of age and older contain two bands/proteins (hereafter referred to as proteins) where only a single Nfasc155 band is expected (between Nfasc186 and Nfasc140) while CST KO mice contain only one. These two proteins are now named "neurofascin 155 high" (Nfasc155H) and "neurofascin 155 low" (Nfasc155L) due to their previous inclusion in a single band.

The western blots shown in Figure 6A (FIGQY primary antibody, which is the antibody used in all subsequent figures, unless otherwise noted) and 6B (NFC1 primary antibody) show only Nfasc155H (with a slight shadow below it) at 15 days of age in both WT and CST KO, with the KO appearing reduced. At 30 days of age, the WT presents Nfasc155H as an intense band with an obvious shadow below while the CST KO shows both Nfasc155H and Nfasc155L with an apparent decrease in the amount of Nfasc155H compared to WT. Seven month old WT mice appear to contain nearly equal amounts of

Figure 6. Extended electrophoresis reveals two bands where only Nfasc155 is expected and only one of these bands appears reduced in the absence of sulfatide. Two bands, now called neurofascin 155 high (Nfasc155H) and neurofascin 155 low (Nfasc155L) are observed when electrophoresis is conducted beyond the usual one hour protocol. In mouse spinal cord (A., B.), the pan-neurofascin antibodies FIGQY (A.) and NFC1 (B.) both demonstrate this novel pattern. The WT and CST KO resemble each other at 15 days of age, but at 30 days of age the WT presents the intense Nfasc155H band with a shadow below while the CST KO shows both Nfasc155H and Nfasc155L at similar intensities. At 7 months of age the WT presents Nfasc155H and Nfasc155L while the CST KO presents virtually no Nfasc155H and approximately normal amounts of Nfasc155L. (C.) Mouse brain homogenates incubated with FIGQY show a similar pattern, except that Nfasc155L is clearly present at 30 days of age in the WT.

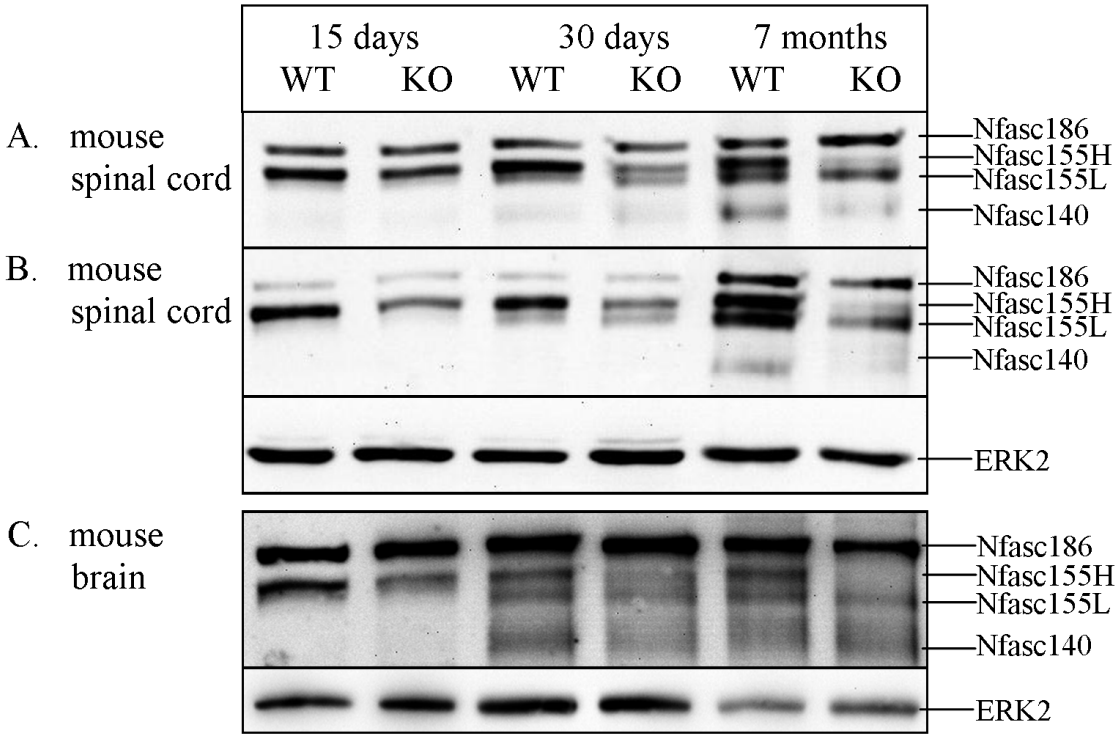

Nfasc155H and Nfasc155L while CST KO mice exhibit almost no Nfasc155H and normal (6A) or reduced (6B) amounts of Nfasc155L. Due to extremely limited amounts of the NFC1 antibody, it was not possible to address this difference directly; however, work to be presented will resolve this difference. Figure 6C shows mouse brain samples incubated with FIGQY and a pattern similar to that seen in the spinal cord. The major difference in the brain is the clear presence of Nfasc155L in the 30 day WT sample. For the remainder of this thesis, "Nfasc155" refers to the protein previously described in the literature and maintained as PubMed Accession AAL27854, Nfasc155 kDa isoform, *Rattus norvegicus*, while "Nfasc155H" and "Nfasc155L" refer to the proteins described here for the first time.

Rats resemble mice regarding Nfasc155H and Nfasc155L

To further understand how Nfasc155H and Nfasc155L change with age, multiple closely aged samples were analyzed. Previous observations suggested that rats, like mice, contain Nfasc155H and Nfasc155L and rats of the desired ages were harvested to evaluate rat as an additional model. As shown in Figure 7A, Nfasc155H increases in intensity from 7 through 27 days of age, decreases between 27 days and 3 months of age, and is maintained between 3 and 5 months of age. Nfasc155L is not observed as a distinct band until 3 months of age and is also observed at 5 months of age. Also similar to mouse, rat spinal cords exhibit a shadow below Nfasc155H at approximately one month of age (30 and 27 days of age in mouse and rat, respectively). A thorough examination of the literature revealed brief mentions (Volkmer *et al*., 1992; Maier *et al*., 2005) and western blot images (Schafer *et*

al., 2004) of a Nfasc155 doublet, with variable glycosylation being suspected as the cause (Maier *et al*., 2005).

PNGase F treatment provides a novel tool to study Nfasc155H and Nfasc155L

Earlier work on the neurofascin proteins indicated that they are glycosylated and respond to treatment with PNGase F, an enzyme that specifically removes N-linked carbohydrates from proteins (Volkmer *et al*., 1992; Davis *et al*., 1993). Based on the results shown in Figures 6 and 7A, it was hypothesized that Nfasc155H and Nfasc155L were the same polypeptide with varying amounts of N-linked glycosylation and that treatment with PNGase F would result in the collapse of the two bands into one "smaller" band. This hypothesis is consistent with previous finding with the two glycoforms of contactin, the proposed binding partner of Nfasc155 (Bonnon *et al*., 2003). Figure 7B shows rat spinal cord samples from various ages after treatment with PNGase F. Foremost, Nfasc155H and Nfasc155L did not collapse into one band following treatment and each band was not only maintained but better separated and therefore more clearly visible. Accordingly, PNGase F was utilized in many other parts of this study. This observation suggests that these two proteins are unique based on differences other than N-linked glycosylation. Additionally, the 7 day old spinal cord contains barely detectable Nfasc155H (Figure 7B) and the level increases steadily with age between 7 and 27 days of age, resulting in an approximately four fold increase (as determined by densitometry). Between day 27 and 3 months of age Nfasc155H levels are reduced by approximately 50% and are then maintained between 3 and 5 months of age. This profile coincides with myelination (Collinson *et al*., 1998);

Figure 7. Nfasc155H and Nfasc155L are developmentally regulated. Rat spinal cord samples are shown from various ages, demonstrating the relative changes in the amount of each protein with age. (A.) Extended electrophoresis shows steadily increasing amounts of Nfasc155H from 7 to 27 days of age followed by a reduction by 3 months of age. Nfasc155L, first visibly distinct at 3 months of age, appears to form from the shadow below Nfasc155H at 21 and 27 days of age. (B.) PNGase F treatment of the same samples reveals onset of Nfasc155L between 7 and 14 days of age. Nfasc155H reaches peak levels at 27 days of age while Nfasc155L continues to increase in abundance up to 5 months of age. While Nfasc155H is more abundant from 7 to 27 days of age, Nfasc155L is more abundant than Nfasc155H at 3 and 5 months of age.

A. Rat spinal cord

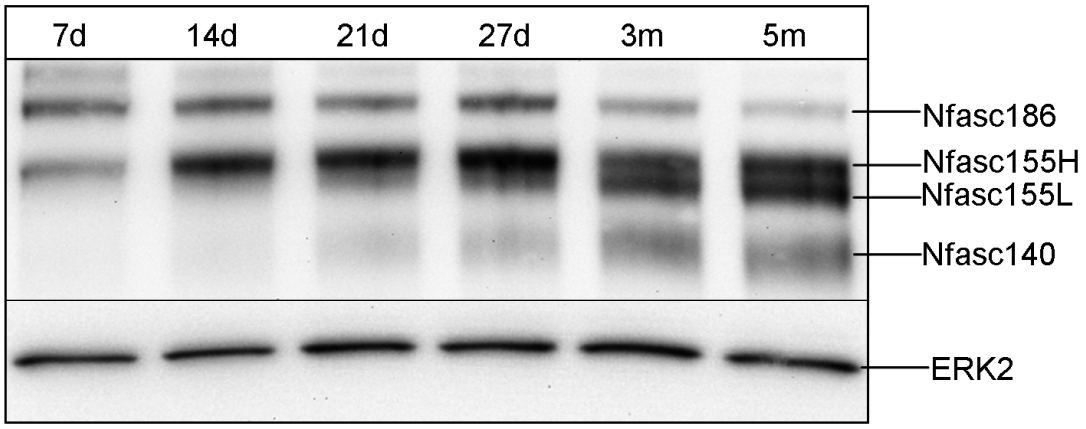

B. Rat spinal cord, PNGase F treated

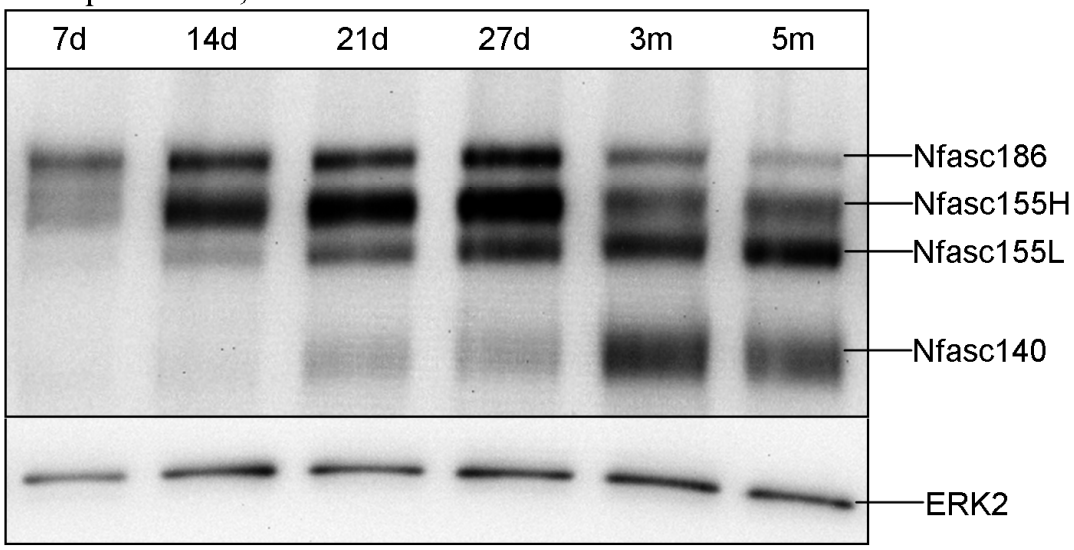

however, levels of major myelin proteins are maintained after myelination peaks (Coetzee *et al*., 1998). Nfasc155L is not detected at 7 days of age, increases steadily with age thereafter, and appears more abundant that Nfasc155H at 3 and 5 months of age. Of the ages examined, 5 months shows the highest level of Nfasc155L. Interestingly, without PNGase F, Nfasc155L is not clearly observed until 3 months of age (Figure 7A) while with PNGase F it is observed by 14 days of age (Figure 7B).

Nfasc155H clusters at the paranode

The observation that Nfasc155H, and not Nfasc155L, is present at 7 days of age provided a unique age at which to evaluate the localization of Nfasc155H. Immunohistochemistry of a 7 day old rat spinal cord double labeled with FIGQY and anti-Caspr antibodies shows intense Caspr reactivity at the paranode and FIGQY reactivity at the paranode and node (Figure 8). Labeling of the node with FIGQY is consistent with the distribution of Nfasc186 (Davis *et al*., 1996; Schafer *et al*., 2004) and the paranodal labeling is likely Nfasc155H (Tait *et al*., 2000; Howell *et al*., 2006).

Nfasc155H is specifically altered in the absence of sulfatide

To further analyze the differences between WT and CST KO mice of varying ages, as observed in Figure 6, PNGase F was employed. Figure 9 presents 15 day, 30 day, and 4 month old mouse spinal cord homogenates treated with PNGase F and run alongside untreated controls. No difference was observed between 3, 4, 7, and 9 month old mice regarding Nfasc155H and Nfasc155L patterns.

Figure 8. Nfasc155H localizes to and clusters in the paranode. At 7 days of age, when Nfasc155H is observed via western blot and Nfasc155L is not yet present, the pan-Nfasc antibody FIGQY (green) labels the node (presumably Nfasc186) and the paranode (most likely Nfasc155H) in rat spinal cord. Anti-Caspr defines the paranode (red) and node (blank region between the red regions). The merged image shows Nfasc155H and Caspr as orange, representing the paranode, and Nfasc186 as green, representing the node. Magnification bar = 5μm

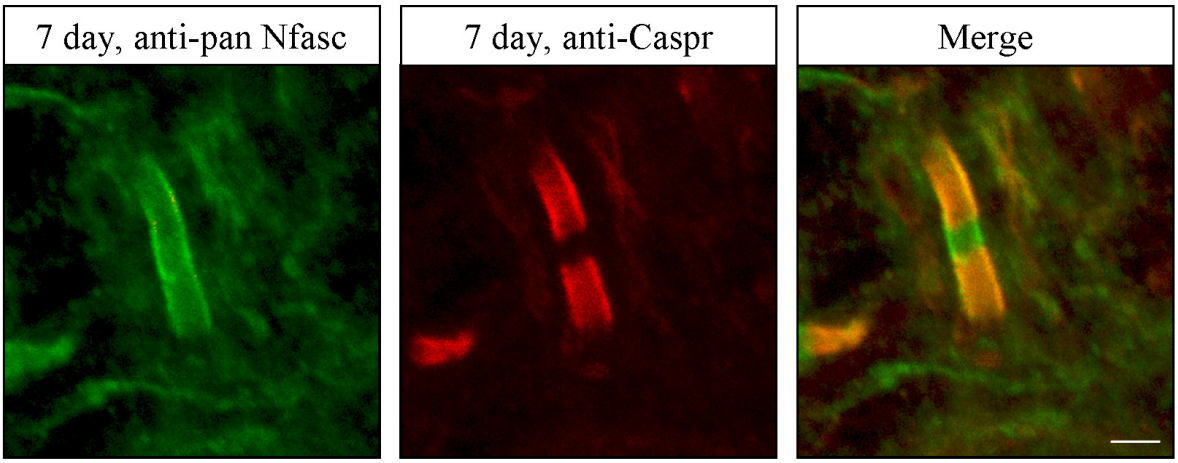

Two important points were made by this experiment. First, Nfasc155H, but not Nfasc155L, is specifically reduced in the absence of sulfatide. Second, while it is not known with absolute certainty that the band labeled "Nfasc155L" in the PNGase F treated 15 and 30 day old WT samples is the same protein seen in the 4 month old WT and KO (untreated and treated), and seen in Figure 7, a systematic evaluation provides strong evidence that they are the same. The 4 month old WT shows three major bands (Nfasc186, 155H, 155L) with and without PNGase F, while the 4 month old CST KO shows only two major bands (Nfasc186, 155L) with and without PNGase F (Figure 9). This indicates the locations (on the blot) of Nfasc186, Nfasc155H, and Nfasc155L after treatment with PNGase F and allows extrapolation to the younger WT mice, confirming the presence of Nfasc155L (as defined by location on the blot at 4 months of age) at 15 and 30 days of age and in both WT and CST KO.

The source of Nfasc155L in the 15 and 30 day old animals has been analyzed in two ways. Density measurements of the Nfasc186 band in all lanes, untreated and PNGase F treated, strongly suggest that Nfasc186 simply shifts following treatment and does not contribute to the intensity of any other band. Additionally, density measurements of the robust band labeled "Nfasc155H" in the 15 and 30 day old untreated WT samples are less than 10% different from the sum of the proposed Nfasc155H and Nfasc155L observed following PNGase F treatment. This is consistent with the band labeled "Nfasc155L" in the 15 day old WT PNGase F treated lane being derived from within the robust band labeled "Nfasc155H" in the 15 day old WT untreated lane. Furthermore, these results suggest that

Figure 9. Nfasc155H, but not Nfasc155L, is dramatically reduced in the absence of sulfatide. Untreated and PNGase F treated homogenates from mouse spinal cords of various ages reveal that Nfasc155H is reduced in the CST KO mice while Nfasc155L levels are comparable to age-matched WT. At 15 and 30 days of age, Nfasc155L (in the PNGase F treated lanes) appears to have come from the shadow below Nfasc155H (in the untreated lanes). Most interestingly, at 4 months of age the CST KO shows no Nfasc155H (arrow). This same result has been observed at 3, 7, and 9 months of age while these mice survive to 15 months of age. WT- = WT untreated, WTP = WT PNGase F treated, KO- = CST KO untreated, KOP = CST KO PNGase F treated

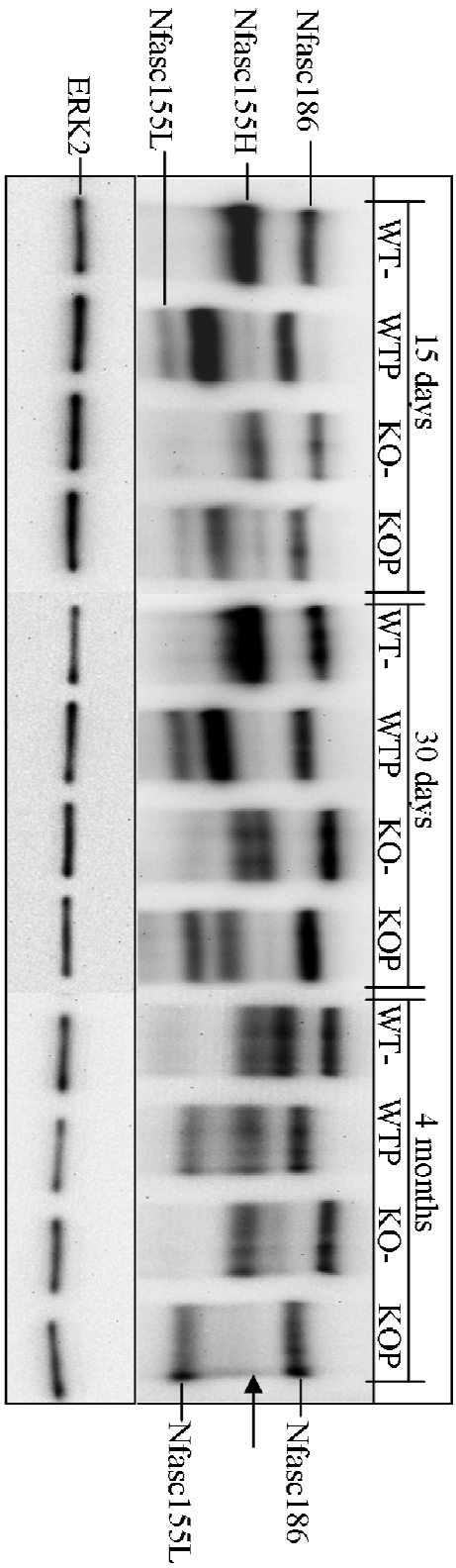

Nfasc155L is somehow masked in untreated younger animal samples, perhaps by the more abundant Nfasc155H or perhaps by subtle changes in N-linked glycosylation with age causing it to migrate closer to Nfasc155H in younger animals, consistent with Figure 7.

Nfasc155L contains more N-linked glycosylated sites than does Nfasc155H

Molecular mass comparisons between untreated and PNGase F treated lanes in animals over 1 month of age were standardized to an immunoladder revealing a 12 kDa shift for Nfasc155H and a 17 kDa shift for Nfasc155L (Figure 9). This 5 kDa difference suggests either more sites of N-linked glycosylation or more extensively glycosylated sites for Nfasc155L. Additionally, analysis with NetNGlyc 1.0 Server predicts five highly likely and two somewhat likely sites of N-linked glycosylation for rat Nfasc155, consistent with multiple sites suggested by the western blot-derived data. Analysis of the apparent molecular masses of Nfasc155H and Nfasc155L shows that after treatment with PNGase F both proteins migrate above 132 kDa, the predicted amino acid mass of Nfasc155, indicating the likely presence of other post-translational modifications and demonstrating that components other than N-linked glycosylation must account for the difference in the apparent molecular masses of Nfasc155H and Nfasc155L.

Nfasc155H, not Nfasc155L, requires detergents for efficient extraction from CNS tissue

Early in the project it was noticed that tissue samples prepared by different researchers yielded different results regarding Nfasc155H and Nfasc155L migrations patterns,

however the significance of these observations was not readily appreciated. Prior to the discovery of the ability of PNGase F to aid in clearer resolution of Nfasc155H and Nfasc155L, multiple (untreated) samples were run in an attempt to quantify the two proteins for statistical analysis. Figure 10 combines two images designed to analyze Nfasc155H and Nfasc155L levels at 15 (Figure 10A) and 30 days of age (Figure 10B). Samples at each time point were gathered from another researcher in the laboratory and run alongside samples that had already been analyzed. The results did not match previous results and it took time to finally realize why. The other researcher's samples had been homogenized in PBS (all samples to this point were homogenized in RIPA buffer) and unexpectedly showed clear Nfasc155L in WT and CST KO mice at both 15 and 30 days of age. This suggested that Nfasc155L is present in the spinal cord of WT mice at 15 and 30 days of age but that, for unknown reasons, it was not visible in the RIPA samples. Additionally, much of the Nfasc155H appeared to be absent from the PBS homogenized samples at both ages.

To answer the question of why PBS and RIPA homogenized samples gave different results required a novel experimental approach. To understand this difference, (WT) tissue was harvested and specifically homogenized in either PBS or RIPA, treated with PNGase F, and the western blot-derived densities of Nfasc155H and Nfasc155L compared. Figure 11 is derived from one adult rat; its brain was cut in half longitudinally, with one half homogenized in RIPA and the other half in PBS. The same procedure was carried out on

Figure 10. RIPA and PBS homogenized spinal cords show different patterning of Nfasc155H and Nfasc155L at 15 and 30 days of age. Attempts to quantify the differences observed between WT and CST KO mice were halted when it was realized that RIPA and PBS homogenized samples give different results. (A.) 15 day old WT spinal cords homogenized in PBS show less Nfasc155H compared to samples homogenized in RIPA and Nfasc155L is unexpectedly visible in the PBS WT samples. RIPA and PBS homogenized 15 day old CST KO samples are indistinguishable. (B.) At 30 days of age, PBS WT samples exhibit less Nfasc155H than the RIPA WT, while the RIPA WT shows intense Nfasc155H with a shadow below. Surprisingly, Nfasc155L is clearly visible in the PBS WT lanes. Similar to the 15 day old spinal cords, RIPA and PBS homogenized CST KO are indistinguishable at 30 days of age. The unexpected results of less Nfasc155H and visible Nfasc155L in PBS homogenized samples at both ages led to further evaluation of the differences between RIPA and PBS.

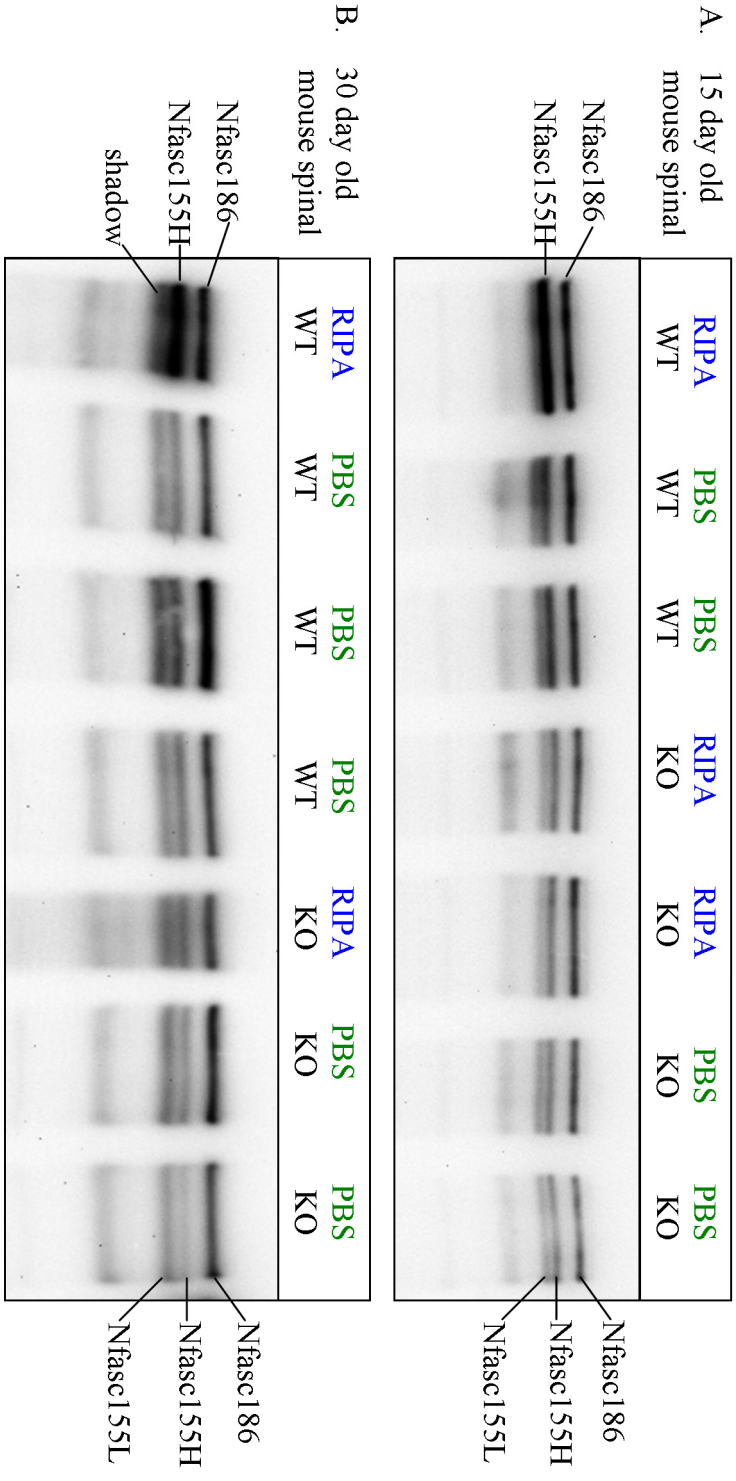

the spinal cord. As expected, the detergent-containing RIPA buffer extracts more total protein (as per the protein assay) than the detergent-lacking PBS (62% less in the brain and 64% less in the spinal cord). To account for this reduction in protein and allow for comparisons between RIPA and PBS, the densitometry of each RIPA band was reduced by the appropriate percentage. Only the PNGase F treated lanes were compared and RIPA bands were assigned to 100%. Figure 11 shows that PBS extracts only 4% of Nfasc155H from brain (see example calculation below *) and 55% from the spinal cord of an adult rat. In contrast, Nfasc155L is more readily extracted without detergents; yielding 100% from brain and spinal cord (118% and 174% respectively, indicating that Nfasc155L comprises a larger portion of the total protein population in PBS compared to RIPA, similar to ERK2, data not shown). These differences demonstrate varying extractabilities of the two proteins, with Nfasc155H being less extractable than Nfasc155L, and suggest that different intermolecular interactions regulate the variable localization/functions of Nfasc155H and Nfasc155L. Additionally, Nfasc155H extracts differently from brain and spinal cord, demonstrating varying interactions even within the CNS. These results suggest an explanation of why PBS homogenized samples (Figure 10) previously showed Nfasc155L at 15 and 30 days of age when RIPA did not (Figures 6, 7, 9); in PBS, much less Nfasc155H is extracted while comparable amounts of Nfasc155L are extracted, allowing for visualization of the much less prevalent Nfasc155L. Also of interest, between Nfasc155H and Nfasc155L (following RIPA extraction), Nfasc155H predominates in the brain while similar amounts of the two proteins are extracted from the spinal cord, implying unique, tissue-specific levels.

Figure 11. Nfasc155H, but not Nfasc155L, requires detergents for extraction from brain and spinal cord. RIPA (A.) and PBS (B.) were used to homogenize respective halves of the brain and spinal cord from a 5 month old rat. Untreated (-) and PNGase F treated (P) lanes are shown. The RIPA homogenized samples indicate 100% of each protein and show distinct Nfasc155H and Nfasc155L after treatment with PNGase F. In contrast, Nfasc155H is barely detected after PBS homogenization while Nfasc155L is comparable between PBS and RIPA. This difference is indicative of Nfasc155L being soluble while Nfasc155H likely interacts with other proteins or lipids, resulting in insolubility. Panels A and B are the same western blot, optimized for each set of lanes.

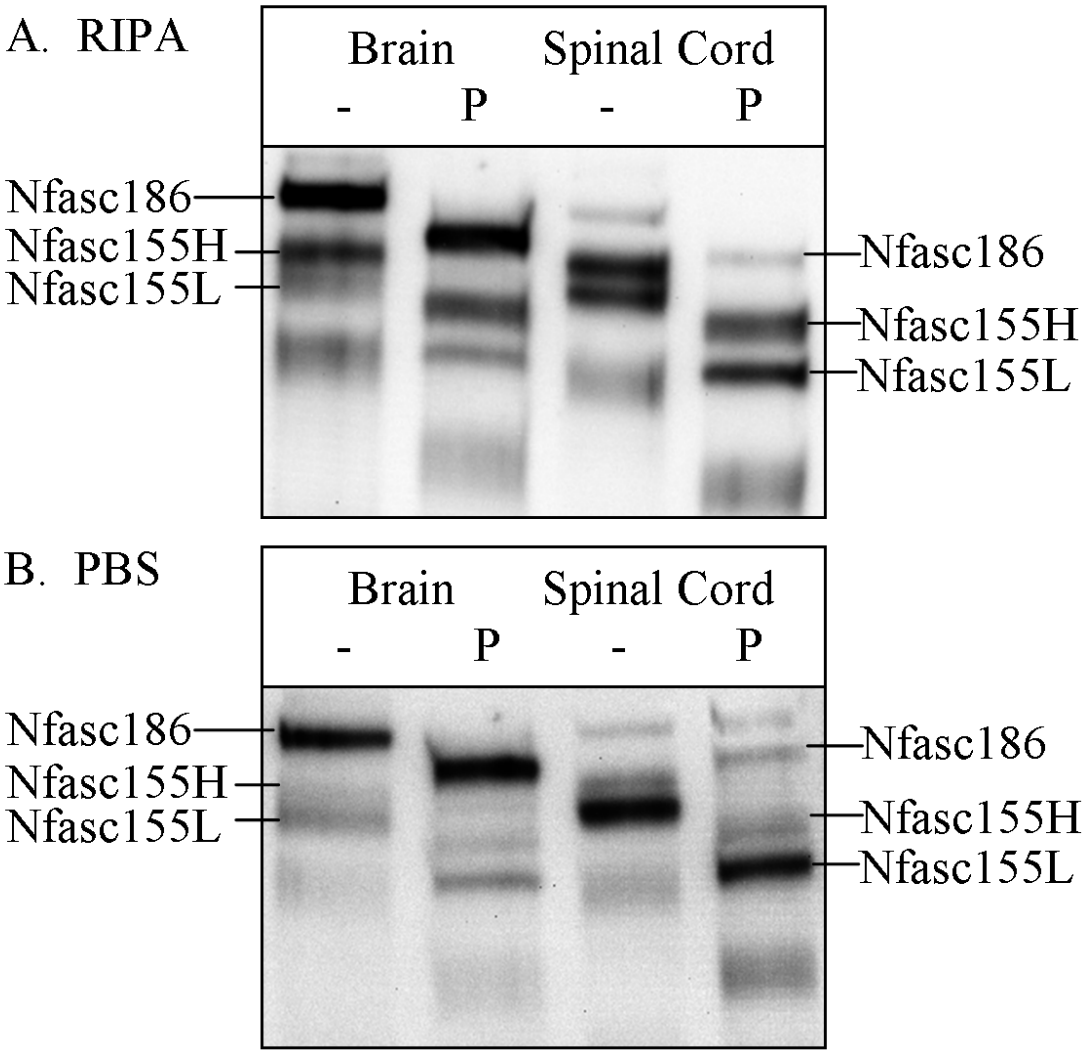

* To calculate brain Nfasc155H (units are density values):
PBS Nfasc155H = 325776
RIPA Nfasc155H = 23111010
RIPA Nfasc155H - 68% = 8782183.8 (corrected RIPA Nfasc155H)
(PBS Nfasc155H / corrected RIPA Nfasc155H) * 100 = 3.7% ~ 4%

Nfasc155H exists as both sulfatide-dependent and sulfatide-independent populations

The data collected thus far regarding Nfasc155H and Nfasc155L indicated that the levels of these proteins are altered in the absence of sulfatide and differ in their detergent-dependent extractabilies. It seemed possible that the detergent-dependent extractabilities may vary in a sulfatide-dependent manner. To test this hypothesis, 15 day old WT and CST KO mouse spinal cords were homogenized in either RIPA (Figure 12A) or PBS (Figure 12B), treated with PNGase F, and band densities compared after western blot. In agreement with data already presented (in Figure 9), the RIPA homogenized CST KO spinal cords contain approximately 68% less Nfasc155H and 34% less Nfasc155L following PNGase F treatment compared to WT. In contrast, the PBS homogenized samples contain very similar amounts of both Nfasc155H (100% in WT, 84% in CST KO; 16% reduced) and Nfasc155L (100% in WT, 88% in CST KO; 12% reduced). A possible explanation for the 68% reduction in RIPA versus the 16% reduction in PBS for Nfasc155H in the CST KO (a 52% change) is that there are two populations of Nfasc155H in WT mice, one that is dramatically decreased in the CST KO (sulfatide-dependent) and requires detergents for extraction and another that is minimally decreased in the CST KO (sulfatide-independent) and completely extracted in PBS. A similar trend was observed for Nfasc155L; however, the difference was much less dramatic.

Figure 12. Nfasc155H exists as both sulfatide-dependant and sulfatide-independent populations. (A.) As already shown, RIPA homogenization shows an approximately 50% reduction in Nfasc155H in the CST KO, compared to WT, while Nfasc155L is minimally altered. (B.) In contrast, the WT and CST KO exhibit the same amount of Nfasc155H and Nfasc155L when homogenized in PBS, consistent with a sulfatide-dependant population of Nfasc155H (altered in the absence of sulfatide, Panel A) and a sulfatide-independent population of Nfasc155H (unaltered in the absence of sulfatide, Panel B).

- = untreated, P = PNGase F treated

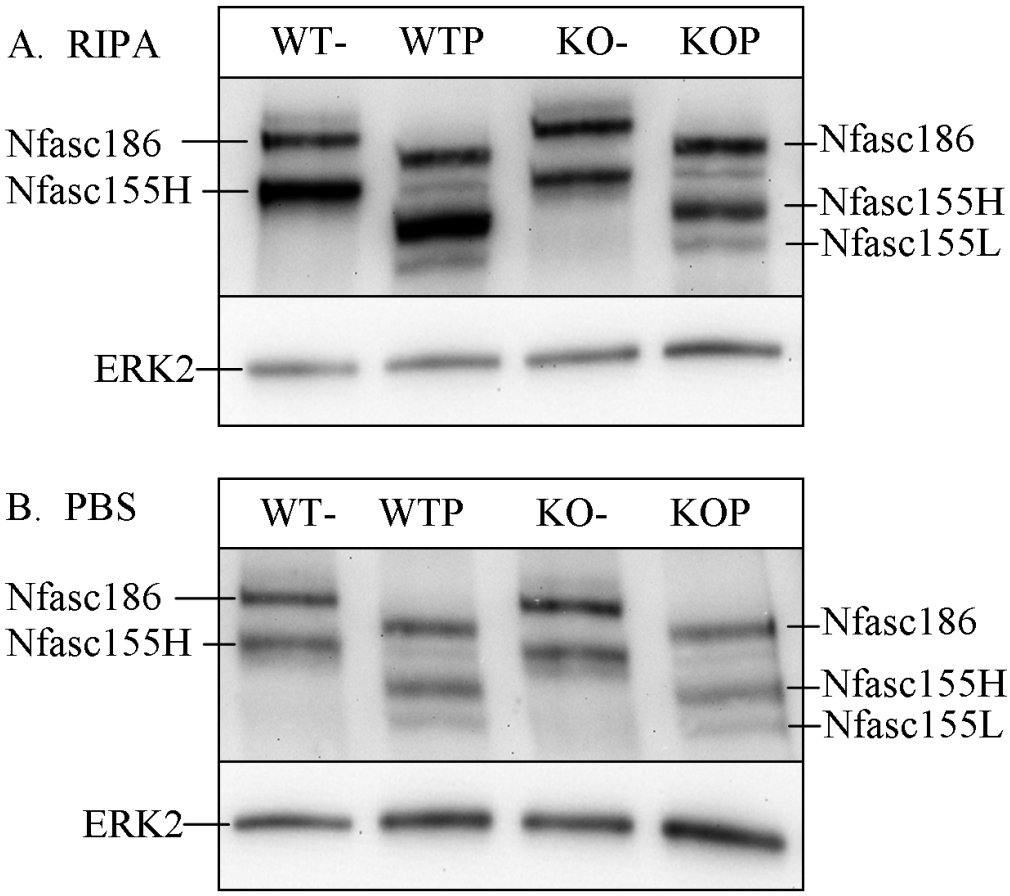

Caspr KO mice resemble CST KO mice regarding Nfasc155H and Nfasc155L

The CST KO mice exhibits altered distribution of Caspr (Ishibashi *et al*., 2002) and Nfasc155 (Marcus *et al*., 2006). Mice mutated within the Caspr gene (Caspr KO) lack Caspr and contactin at the paranode (Bhat *et al*., 2001) and it was hypothesized that the level of Nfasc155H would be disrupted in the Caspr KO mice in a manner similar to the CST KO. The spinal cord of a 19 day old Caspr KO and littermate WT were analyzed by the same western blot/PNGase F methods previously described for the 15 day old CST KO mice already discussed. Figure 13 shows 58% less Nfasc155H and 22% less Nfasc155L in the Caspr KO compared to its littermate WT. These reductions strongly resemble those observed in the 15 day old CST KO spinal cord. Thus, the substantial decrease of Nfasc155H is not specific to an oligodendrocyte defect (CST KO) but appears to be universally related to the loss of paranodal integrity. Although the levels of Nfasc155H display a greater reduction than Nfasc155L in both the oligodendrocyte (CST KO) and neuronal (Caspr KO) mutants, these results do not exclude a role for Nfasc155L as a component of the paranode. However, the more severe loss of Nfasc155H in the absence of sulfatide and Caspr, combined with the findings presented in Figure 8 that Nfasc155H is a component of the paranode, strongly implicate Nfasc155H in the maintenance of paranodal stability.

Nfasc155H and Nfasc155L are altered in multiple sclerosis

As early as 1969 (Suzuki *et al*.), studies demonstrated that paranodal structure is compromised in multiple sclerosis (MS), the most common demyelinating disease of the

Figure 13. Caspr KO mice, similar to CST KO mice, exhibit a dramatic reduction in Nfasc155H. Spinal cords of 19 day old Caspr KO mice (CPKO) were examined by the same PNGase F/extended western protocol already discussed. Similar to the 15 day old CST KO mice, the Caspr KO contains approximately 58% less Nfasc155H and 22% less Nfasc155L than the littermate WT (CPWT). Following treatment with PNGase F, the Caspr KO shows no band representing Nfasc155H, only a diffuse haze (arrow).

- = untreated, P = PNGase F, MM = Magic Mark Western Protein Standard (Invitrogen)

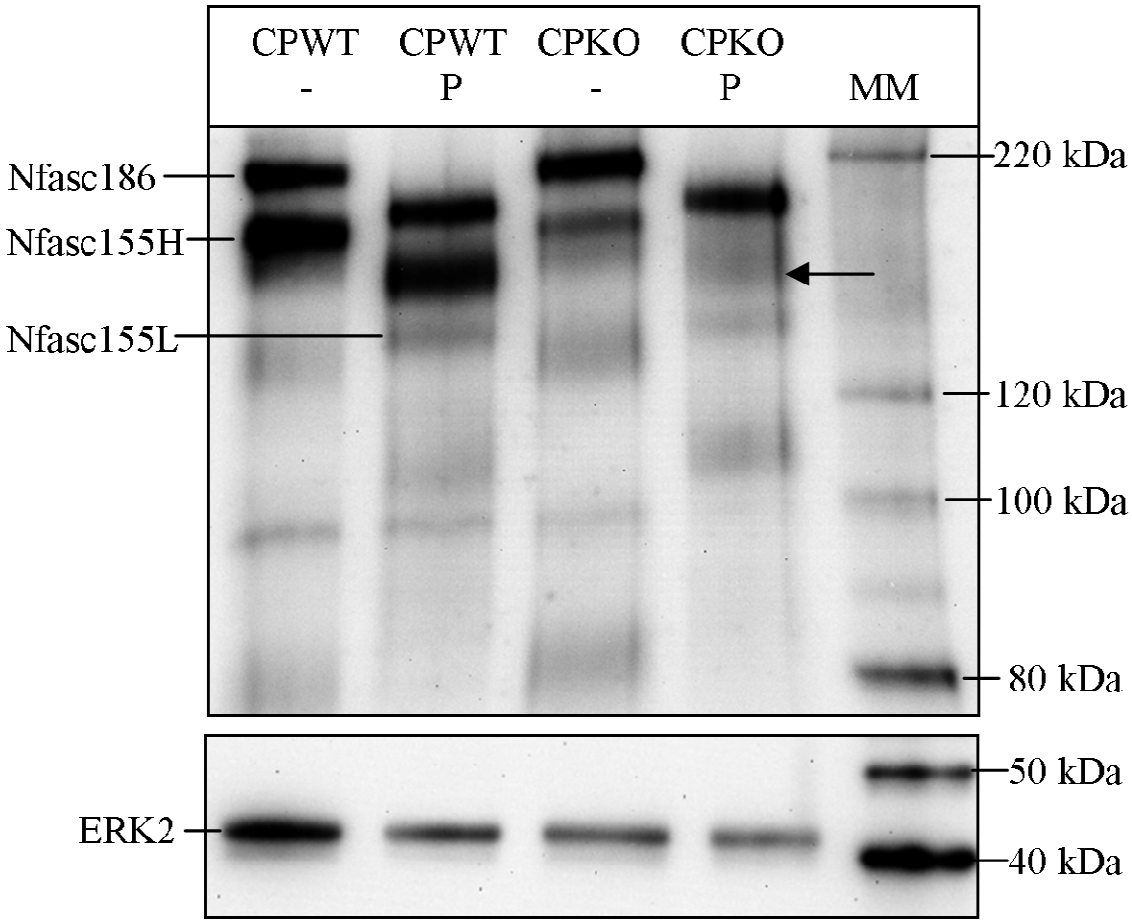

human CNS. It has recently been determined that paranodal integrity is altered in the presence of intact nodes (Wolswijk and Balesar, 2003; Howell *et al*., 2006) in MS tissue. Specifically, Caspr spreads out of the paranode and voltage-gated K^+ channels lose their juxtaparanodal confines while Na^+ channels and Nfasc186 are still observed at the node. Since MS demonstrates abnormal protein domain organization reminiscent of the CST and Caspr KO mice, it was proposed that Nfasc155H would also be altered in MS. Figure 14 shows four non MS, four NAWM, and eight MS brain samples run following the same parameters used to create Figures 6 and 7A. Qualitatively, Nfasc155H appears as an obvious, intense band in each sample while Nfasc155L is visible in two of the MS samples (the second one in each set of four) but not observed in any of the non MS or NAWM samples. The previously mentioned shadow (Figure 7, 14 - 27 days of age) is seen below Nfasc155H in samples from each set, suggesting that Nfasc155L may be present but masked, similar to the rat and mouse samples. Accordingly, PNGase F treatment was conducted on half of each sample set and the results are presented in Figure 15. None of the non MS or NAWM shows distinct Nfasc155L, even after treatment with PNGase F. These samples still display the shadow below Nfasc155H, but this cannot be definitively called Nfasc155L. The prevalent shadow may be low abundance Nfasc155L but this technique does not allow for visualization beyond that which is shown. Figure 15C shows a reduced intensity image of the unexpectedly robust sample from Figure 15B. Of note, the untreated lane shows only one band, seemingly Nfasc155H, while the PNGase F treated lane shows two clear bands, Nfasc155H and Nfasc155L, demonstrating the effectiveness of PNGase F treatment in the detection of Nfasc155L.

Figure 14. Nfasc155H is present in non MS brain while Nfasc155H and Nfasc155L are present in MS brain. A total of four non MS, four NAWM, and eight MS brain samples are shown, and while Nfasc155H is present in all samples, Nfasc155L is only present in two (denoted ★), both of which are MS samples. The shadow seen below Nfasc155H in many of the samples (denoted •) suggests the masked presence of Nfasc155L. MS = multiple sclerosis, NAWM = normal appearing white matter

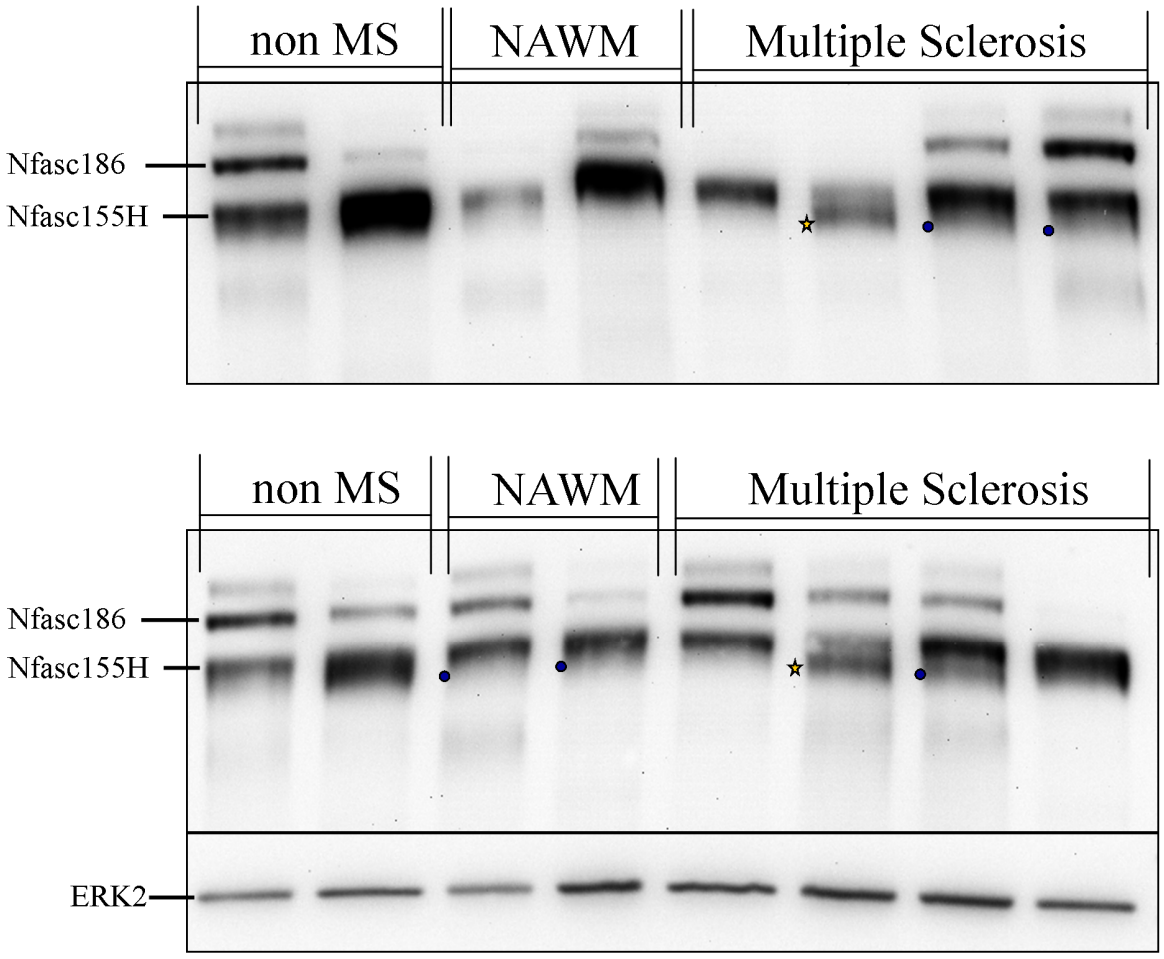

Figure 15. The pattern of Nfasc155H and Nfasc155L is altered in multiple sclerosis. (A.) Non MS and NAWM samples do not exhibit Nfasc155L, even after treatment with PNGase F, while there is still a shadow below Nfasc155H. (B.) Qualitatively, MS samples appear to contain less Nfasc155H than non MS and NAWM samples and Nfasc155L is observed in three of the four MS samples evaluated with PNGase F. (C.) One MS sample is shown at decreased intensity, revealing that while only one band is seen in the untreated lane, both Nfasc155H and Nfasc155L are seen after treatment with PNGase F.

- = untreated, P = PNGase F treated, MS = multiple sclerosis, NAWM = normal appearing white matter

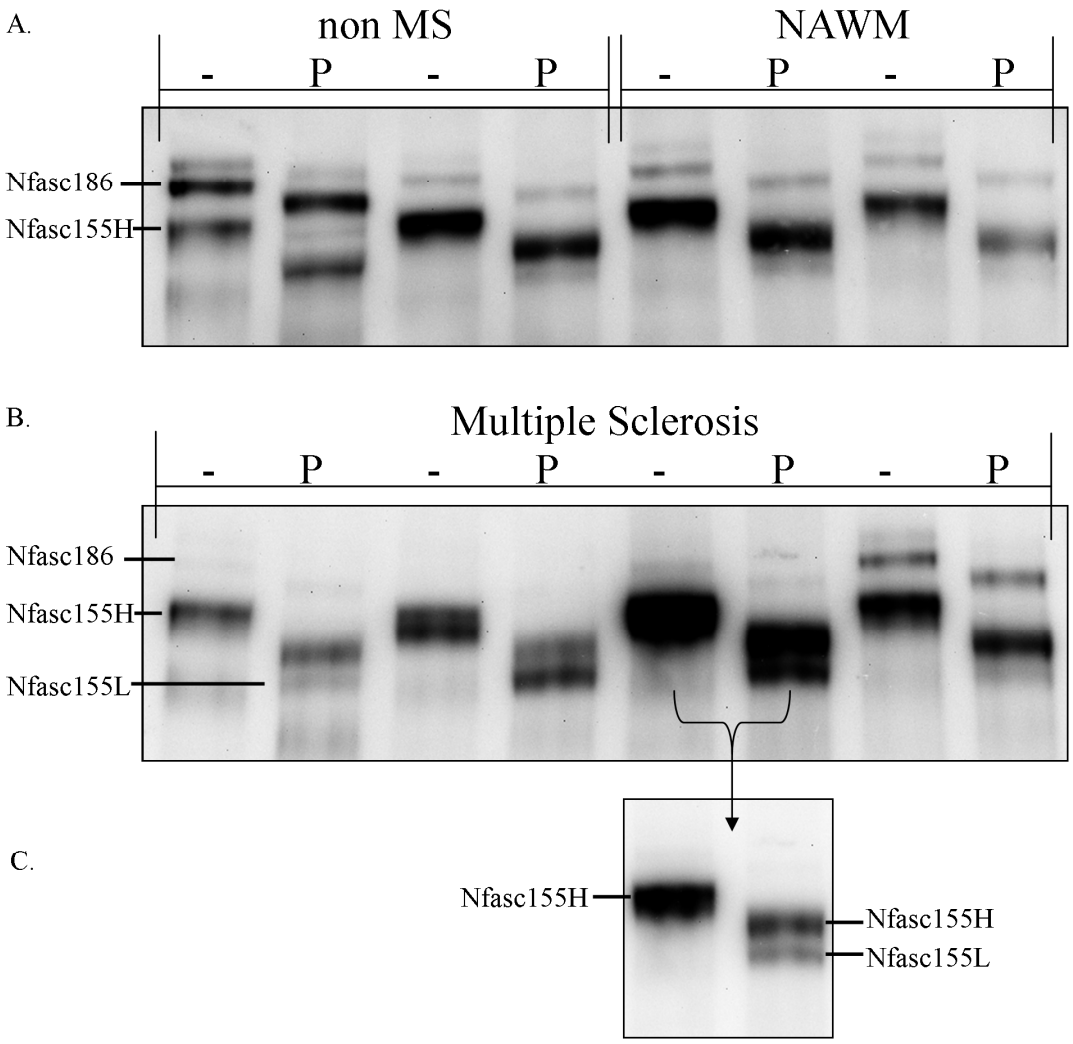

Although non MS spinal cords were not available from the tissue bank, four MS spinal cords were received and analyzed by western blot without (Figure 16A) and with PNGase F (Figure 16B). Without PNGase F, all four MS spinal cords display both Nfasc155H and Nfasc155L. Following treatment with PNGase F, all four MS spinal cords show a higher abundance of Nfasc155L than Nfasc155H. The general pattern observed in the MS spinal cords strongly resembles the pattern observed in the Caspr KO (Figure 13, smeared Nfasc155H with a clear band for Nfasc155L), however, without non MS spinal cord samples, the implications remain unclear.

Attempts to identify Nfasc155H and Nfasc155L were not successful

An important topic that, while addressed, remains unresolved is the amino acid content of Nfasc155H and Nfasc155L. It is still not known whether these two proteins are the same polypeptide with varying post-translational modifications or two unique polypeptides. Mass spectrometry, while not able to provide 100% sequence coverage, could answer this question. The following basic strategy was devised to identify the amino acids present in Nfasc155H and Nfasc155L with mass spectrometry. IP would allow for isolation of neurofascin proteins and these proteins would be separated from each other on a gel and visualized with silver stain. Silver stained bands would be cut out of the gel, destained, and sent to a mass spectrometry facility for identification.

The efforts presented in Figure 17A show that Nfasc155H and Nfasc155L are present in the supernatant of a rat spinal cord before IP, decreased in the supernatant after incubation

Figure 16. MS spinal cords contain Nfasc155H and Nfasc155L. (A.) Only MS spinal cords were available for examination and all four samples show both Nfasc155H and Nfasc155L. (B.) Following treatment with PNGase F, Nfasc155L appears more prevalent than Nfasc155H in MS spinal cords. - = untreated, P = PNGase F treated, MS = multiple sclerosis

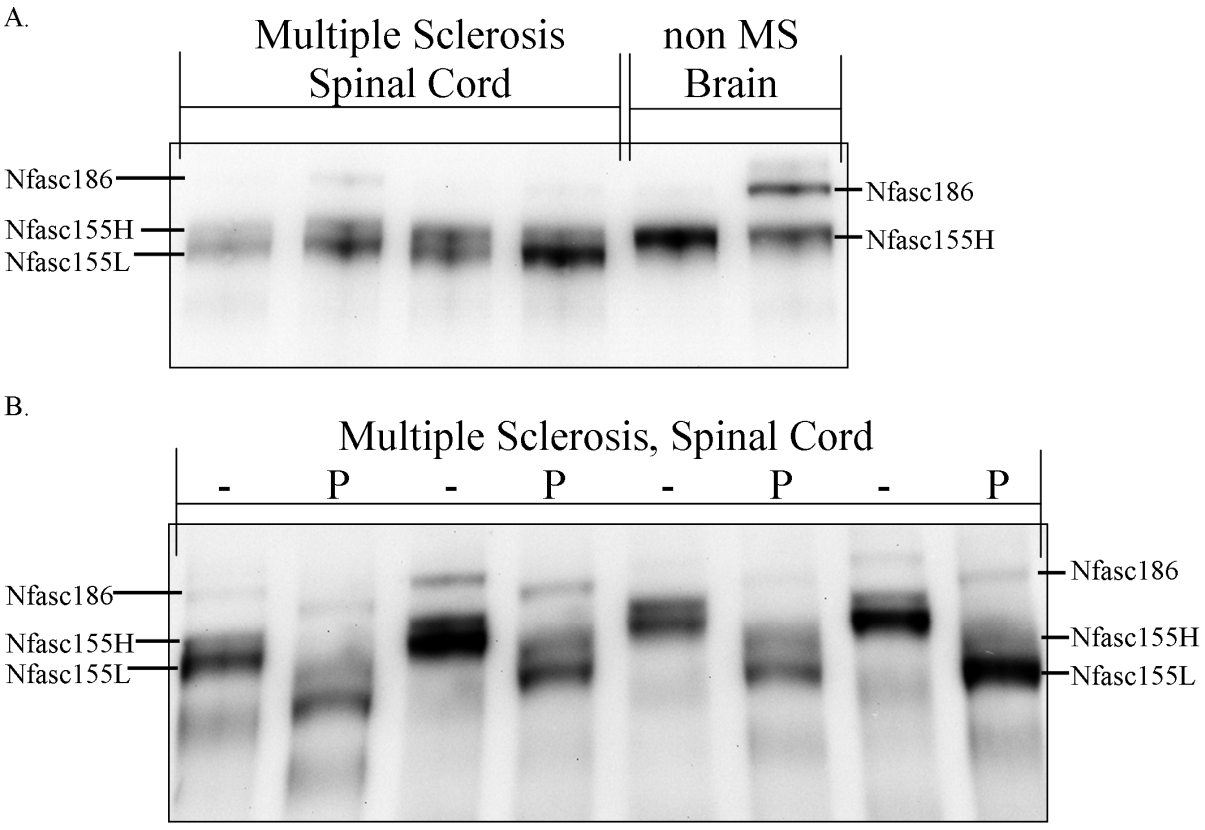

with 10 µL of FIGQY primary antibody, and absent from the supernatant after incubation with another 20 µL of FIGQY primary antibody. To be clear, this was one supernatant, first incubated with 10 µL of antibody, then another 20 µL after realization that Nfasc155H and Nfasc155L had been less than 100% captured by IP. 30 µL of antibody was able to capture all of the Nfasc155H and Nfasc155L from a one-quarter of the supernatant derived from one rat spinal cord. A small fraction of this IP is shown in the fourth lane of the western blot in Figure 17A, demonstrating the success of this portion of the project. Visualization of this IP on a silver stained gel was also successful, as shown in Figure 17A. The intense region labeled "proposed binding complex" was repeatedly observed after IP and is possibly comprised of proteins that bind neurofascin proteins. Upon seeing this silver stain, it was realized that removal of these proteins from the gel without contaminating either protein with trace amounts of the other, thus complicating the mass spectrometry, would be impossible. Thus, the PNGase F technique was applied to the IP, as shown in Figure 17B. The increased separation of the two proteins provided by PNGase F, paired with silver staining should have allowed for confident mass spectrometry of each protein. However, none of the mass spectrometry facilities contacted would attempt to identify silver stained proteins, even those that had been stained with "mass spectrometry compatible silver stain" and destained. The problem, it seemed, was that while silver stained proteins are compatible with mass spectrometry, the process requires large amounts of protein. Only if the proteins of interest are visible with Coomassie stain are they likely to yield a positive result in a mass spectrometer. The main difference between silver stain and Coomassie stain is the sensitivity, with silver stain being dramatically more sensitive.

To remedy this problem, entire spinal cords from adult rats were harvested and subjected to IP with 100 µL of FIGQY, eluted in the buffers required for activity of PNGase F, treated with PNGase F, concentrated in Centricon tubes, and visualized. While this gave beautiful results on western blots (as per Figure 17B), there simply was not enough Nfasc155H or Nfasc155L in one rat spinal cord to be detected by Coomassie. Two sets of silver stained Nfasc155H and Nfasc155L was sent to different mass spectrometry facilities, but no amino acids were identified. Attempts to run IP on multiple rat spinal cords were met with the problem of limited antibody. The FIGQY antibody is not commercially available and was supplied to the laboratory in generous, but limited, amounts by Dr. Matthew Rasband (Baylor College of Medicine). Several hundred µL were consumed and attempts to commit many more hundreds of µL of antibody to this part of the project would have prevented every other part of the project from proceeding forward, including most of the data presented here.

Figure 17. Steps to identify Nfasc155H and Nfasc155L were successfully established, but identification did not occur. (A.) The western blot demonstrates the ability of the FIGQY antibody to remove Nfasc155H and Nfasc155L from a spinal cord homogenate. Increasing the volume of antibody from 10 to 30 μL resulted in complete capture of Nfasc proteins in the IP. A small fraction of the IP is shown to demonstrate the effectiveness of the protocol. The silver stain shows all of the Nfasc155H and Nfasc155L captured from one-quarter of one rat spinal cord homogenate. This was just enough for detection by silver stain and later work showed that one whole spinal cord worth of Nfasc155H and Nfasc155L was not enough to be detected by Coomassie stain. (B.) PNGase F (P) treatment provided further separation of Nfasc155H and Nfasc155L and was intended to allow for confident removal of each band from the gel without cross contamination. A western blot is shown, demonstrating that the IP and PNGase F protocols work in tandem.

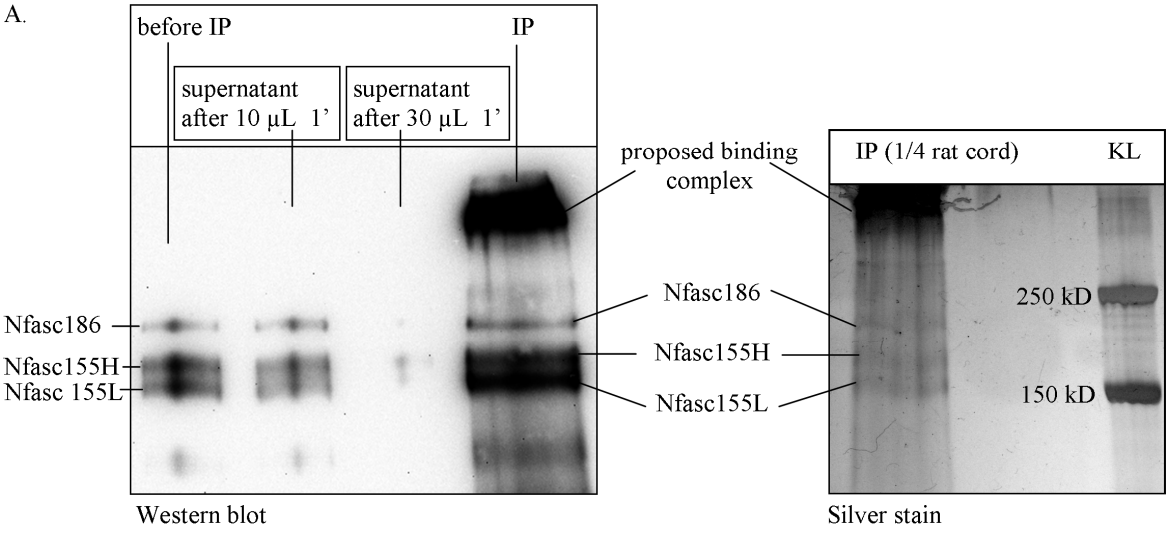

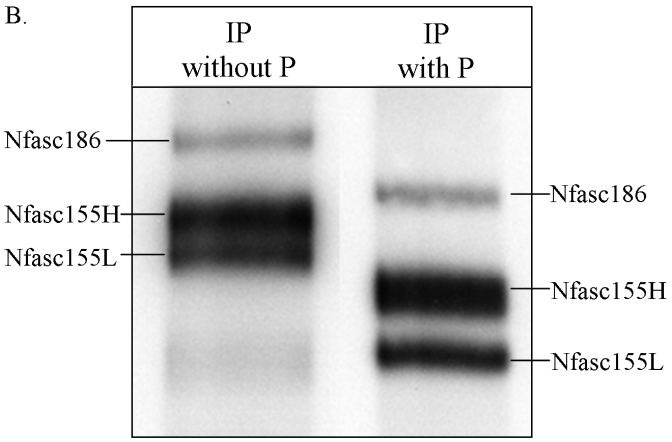

{CHAPTER 4 Discussion}

Nfasc155H is a component of the myelin paranode

Nfasc155H has been shown to increase steadily in abundance in the rat spinal cord between 7 and 27 days of age, a trend consistent with the major myelin proteins during myelination in the rat spinal cord (Yanagisawa *et al*., 1986). However, Nfasc155H abundance decreases between 27 days and 3 months of age while Coetzee and colleagues (1998) have shown that myelin protein levels remain constant between 30 and 90 days of age, suggesting that Nfasc155H may play variable roles in myelination and myelin maintenance. Additionally, it has been shown here that Nfasc155H localizes to the paranode in the spinal cord of a 7 day old rat, consistent with Tait and colleagues (2000) who showed, with immunoelectron microscopy, that the NFC1 antibody (shown here in Figure 6B) labels the point of contact between the paranodal loops of myelin and the axon. Nfasc155 has been previously shown to be expressed only by oligodendrocytes (Collinson *et al*., 1998) and it is therefore concluded that Nfasc155H is an oligodendrocyte-specific protein and a component of the myelin paranode.

Nfasc155L as a myelin component

Nfasc155L is first detected on a western blot by 14 days of age in the rat spinal cord then gradually increases in abundance up to 5 months of age and is more abundant than Nfasc155H at 3 and 5 months of age. The lack of Nfasc155L-specific antibodies is a hindrance to the identification of the cell of origin and location of Nfasc155L; however,

inferences can be made based on the data presented here. Figure 11A shows that there is more Nfasc155L in 25 µg of spinal cord homogenate than in 40 µg of brain homogenate, demonstrating white matter-enrichment for Nfasc155L. Additionally, published (Marcus *et al*., 2006) and unpublished (Shepherd *et al*., manuscript in progress) observations from this laboratory reveal that the thickness of the myelin sheath increases throughout life, resulting in paranodal loops that form stacks above the traditional paranode and do not contact the axon. The increasing abundance and white matter-enrichment of Nfasc155L combined with the increasing thickness of myelin and number of paranodal loops through life is consistent with a role for Nfasc155L in the maintenance of mature myelin sheaths. Nfasc186 (Davis *et al*., 1993) and Nfasc155 (Gollan *et al*., 2003) have each been shown to bind homophilically in *trans,* consistent with the hypothesis that Nfasc155L maintains homophilic interactions across (in *trans*) lamellae in the same myelin sheath and suggesting a reason for the increasing abundance of Nfasc155L with age. Specifically, as myelin becomes thicker and thicker with age, Nfasc155L expression may be up regulated to aid in maintaining the stability of successive lamellae in the absence of axonal contact. It is therefore proposed that Nfasc155L is a highly glycosylated transmembrane protein and a component of the myelin sheath involved in myelin:myelin cohesion. Similarly, the Ig Superfamily member myelin-associated glycoprotein (MAG), is located at various points in the myelin sheath and expressed as two alternatively spliced, similarly sized, developmentally variable isoforms (Trapp *et al*., 1989) with no known *in vivo* binding partners; however see Shelke *et al*., 2007.

Nfasc155H and Nfasc155L are differentially glycosylated

Treatment of homogenates from animals over one month of age (when both Nfasc155H and Nfasc155L are clearly visible) with PNGase F results in shifts of 12 and 17 kDa for Nfasc155H and Nfasc155L, respectively. Based on each site representing approximately 2.5 kDa, these shifts are consistent with the NetNGlyc Server 1.0 prediction for rat Nfasc155, which predicts five highly likely and two somewhat likely sites of N-linked glycosylation (see Materials and Methods for definitions). Furthermore, this difference in N-linked glycosylation suggests either a protein domain unique to Nfasc155L or distinct glycosylation of Nfasc155H and Nfasc155L, perhaps due to different cellular or subcellular localizations. Since both proteins are visible as distinct bands before and after PNGase F treatment (did not collapse into one band), they likely differ in either another post-translational modification and/or amino acid content.

Nfasc155L is alternatively glycosylated with age

Experiments with PNGase F demonstrate that Nfasc155L is present in WT rat spinal cords as young as 14 days of age, while Nfasc155L is not observed until 3 months of age in untreated samples. In these untreated samples, Nfasc155L seems to gradually form from the shadow below Nfasc155H between 14 and 27 days of age (Figure 7), suggesting that Nfasc155L becomes alternatively glycosylated with age, causing it to migrate with Nfasc155H in young animals and lower than Nfasc155H in older animals. Supportive of this idea, both Nfasc155H and Nfasc155L shift following treatment with PNGase F, with Nfasc155L more so than Nfasc155H at older ages (over 30 days of age) while the shift is

not measurable in younger animals due to the undefined location of Nfasc155L in non-PNGase F treated young samples. Presumably, Nfasc155L is migrating at almost exactly the same rate as Nfasc155H in young animals (day 14), and an extrapolation can be made that the shift from untreated Nfasc155H+L to PNGase treated Nfasc155L is 22 kDa. This is 5 kDa more than the 17 kDa shift reported here for Nfasc155L in older animals, indicative of approximately two more sites of N-linked glycosylation for Nfasc155L in younger (14 - 30 days old) compared to older animals. It is reasonable to believe that Nfasc155L gradually loses two N-linked glycosylations with age, accounting for the increasingly dark shadow below Nfasc155H that gives rise to distinct Nfasc155L at 3 months of age. Alternative glycosylation of proteins in the context of cellular maturation has been previously demonstrated for Ig Superfamily members in the immune system (reviewed by Daniels *et al*., 2002). This alternative glycosylation with age may be involved in the proposed *trans* homophilic interactions of Nfasc155L. CST KO mice appear to properly follow this age-dependent change in glycosylation, with Nfasc155L being present and in approximately normal amounts at all ages examined.

Is the specific reduction of Nfasc155H in paranodal mutants due to improper interactions at the myelin paranode?

Analysis with PNGase F reveals that sulfatide null spinal cords contain ~50% less Nfasc155H than littermate WT at 15 days and 30 days and nearly 100% less at 4 months of age (Figure 9). Similarly, Nfasc155H is reduced ~70% in the spinal cord of the 19 day old Caspr KO mouse. In both CST and Caspr KO spinal cords, Nfasc155L content is

minimally altered. Since evidence presented here strongly indicates that Nfasc155H is a paranodal component, the near complete loss of Nfasc155H by 4 months of age likely explains the near complete loss of anti-Nfasc reactive paranodes in older CST KO mice (Figure 4C, Marcus *et al*., 2006).

In addition to the immunohistochemistry presented in Marcus *et al*. (2006), this laboratory has since quantified paired paranodal clusters at 15 and 30 days (Pomicter *et al.,* manuscript in progress). Compared to littermate WT, CST KO spinal cords contain ~50% and 90% fewer paired paranodal clusters (defined by reactivity with the NFC1 antibody) at 15 and 30 days of age, respectively. It is interesting to note that paired paranodal clusters are not simply altered in the absence of sulfatide; they are *increasingly* altered in the absence of sulfatide. The results of the western blot in Figure 9 shows that Nfasc155H is reduced ~50% at both ages, indicating that the 90% reduction in paired clusters observed at 30 days of age is likely due to improperly localized, and therefore undetectable, Nfasc155H. This demonstrates that even in the presence of Nfasc155H, paired paranodal clusters are formed but not maintained in the absence of sulfatide.

The CNS of the CST KO mouse contains normal amounts of mRNA for PLPs, MBPs, and MAGs (Honke *et al*., 2002) as well as normal amounts of proteins for MBPs, and CNPs (presented here) at various ages, strongly suggesting that transcription and translation are unaltered in oligodendrocytes by the absence of sulfatide. If the transcription and translation of Nfasc155H are also unaltered in the CST KO, then protein stability could

account for the reduction in Nfasc155H at each age examined; leading to the question, "Why is only Nfasc155H reduced in the absence of sulfatide?".

A leading explanation can be drawn from comparisons between PBS and RIPA homogenized tissue, which demonstrates that Nfasc155L is extracted in the absence of detergent. This is consistent with Nfasc155H being the protein studied by Schafer and colleagues (2004) since fractionation based on solubility was their first step and the high solubility of Nfasc155L (shown here) excludes it from their study. The authors describe Nfasc155 as having characteristics consistent with lipid raft/membrane microdomain incorporation and it is proposed here that they were examining only Nfasc155H. This may help to explain why Nfasc155H is so dramatically altered in the sulfatide null mice. Arvanitis and colleagues (2005) have shown that sulfatide (cerebroside sulfate) is enriched in a specific fraction of isolated myelin that also contains enrichments of the lipid raft proteins fyn (Krämer *et al*., 1999), flotillin-1 (Salzer *et al*., 2001), and caveolin (Sargiacomo *et al*., 1993). This enrichment demonstrates a relationship between sulfatide in myelin and specific membrane microdomain-associated proteins, with Nfasc155H at the myelin paranode seemingly being one of them. Loss of sulfatide will compromise this interaction, allowing for altered localization (as shown by Marcus *et al*., 2006, see Figure 3C), loss of any/all intracellular/extracellular binding, and perhaps eventual degradation of Nfasc155H.

Similarly, in the absence of Caspr, the amounts of PLPs, MBPs, and contactin proteins are unaltered (Bhat *et al*., 2001). The Caspr KO mouse shows no band representing Nfasc155H at 19 days of age (Figure 13), suggesting that Nfasc155H is either not transcribed/translated or abnormally degraded in the absence of its *trans* binding complex. Since it is unlikely that Caspr regulates the transcription/translation of Nfasc155H (the two proteins being transmembrane and in different cells) and since other myelin proteins are translated normally, the implication is that Nfasc155H is abnormally maintained in the absence of Caspr. Altered interactions at the paranode may then result in exposure to degradative pathways not normally accessible to Nfasc155H, similar to what has been proposed in the absence of sulfatide.

Nfasc155H and Nfasc155L likely differ in amino acid content

Nfasc155H and Nfasc155L differ by ~10 kDa following removal of N-linked carbohydrates; a difference not easily accounted for by other post-translational modifications. Phosphorylation, the most widely studied post-translation modification (Sims and Reinberg, 2008), for example, has been described as a predominantly intracellular modification and results in minimal changes in the apparent molecular mass of a protein. Specifically, 13 phosphate groups (~95 Daltons each) on a 25 kDa protein changes the apparent size by less than 3 kDa (Gingras *et al*., 1998). The Nfasc cytoplasmic domain is comprised of less than 130 amino acids and contains only ~20 total serines, threonines, and tyrosines (Davis *et al*., 1993), whereas ~44 phosphorylations would be required to constitute 10 kDa (3 kDa/13 sites = 0.23 kDa/site; 10 kDa/(0.23 kDa/site) = 44

sites). This does not, however, rule out phosphorylation as a contributor to the size difference, and Nfasc155 has been indirectly suggested to be phosphorylated at one intracellular site (Garver *et al*., 1997; Jenkins *et al*., 2001).

A recently discovered post-translational modification is the addition of the peptide named small ubiquitin-like modifier and known as SUMO. The addition of a SUMO is termed SUMOylation and is the addition of a 10 kDa (Braun *et al.,* 2008) peptide to a lysine in the following sequon: large hydrophobic amino acid, lysine, any amino acid, glutamic acid. This modification has been shown to be mostly involved in chromatin organization, transcription, and RNA metabolism (reviewed by Hay, 2005) and, while the size fits the difference between Nfasc155H and Nfasc155L, the functions prescribed to SUMOylated proteins do not fit any of the known functions for Ig Superfamily proteins (Salzer, 1995).

Other potential post-translational modifications that might account for or contribute to the 10 kDa difference observed between Nfasc155H and Nfasc155L following removal of N-linked carbohydrates with PNGase F are similar to phosphorylation in that they do not add enough mass to the peptide to make a shift observable on a western blot unless dozens of groups are added. This includes methylation (~15 Daltons), sulfation (~96 Daltons), acetylation (~43 Daltons), and various lipid additions (palmitic acid is ~256 Daltons and myristic acid is ~228 Daltons). The contribution of charged post-translational modifications to gel migration is difficult to account for, but as shown for negatively charged phosphorylation, requires numerous sites to change the apparent molecular mass

of a protein.

Additionally, while mass spectrometry did not provide information regarding specific peptides present in Nfasc155H and Nfasc155L, detailed analyses of the results presented in this thesis provide evidence to suggest that protein domain content accounts for the difference between the two proteins. Nfasc186 appears unaltered in the absence of sulfatide at all ages evaluated and was not the focus of this study. Nonetheless, data regarding Nfasc186 has been accumulated due to the shared cytoplasmic domain targeted by the NFC1 and FIGQY antibodies. Of this data, the most interesting point is that Nfasc186 shifts only 9 kDa following PNGase F treatment, making Nfasc155H and Nfasc186 ~30 kDa different in apparent molecular mass after the removal of N-linked carbohydrates. What then accounts for the difference in the apparent molecular masses of Nfasc155H and Nfasc186? As previously stated, Nfasc155 and Nfasc186 differ in protein domain make up regarding the three insert domains, the 3rd FNIII domain (Nfasc155 only), and the mucin-like/PAT domain (Nfasc186 only). Calculations with the ExPASy Compute pI/MW tool show that Nfasc155 and Nfasc186 differ by no more than 8 kDa, with Nfasc186 being more massive. Evaluation of this apparent discrepancy points toward the 5th FNIII (10.2 kDa) domain being present in Nfasc186. Recall that this domain exists in the Nfasc gene and has been observed in cDNA (Hassel *et al.,* 1997) but that its presence in Nfasc proteins has never been evaluated. Additionally, other L1 subfamily members, including L1 and NrCAM, contain a 5th FNIII domain (Hassel *et al*., 1997). Analysis of the 5th FNIII domain with the NetNGlyc 1.0 Server predicts three sites of N-linked

glycosylation (more than any other Nfasc domain), including one somewhat likely, one highly likely, and one extremely likely site of N-linked glycosylation (the only extremely likely site in all of the possible Nfasc domains, 9/9 neural networks agree, + + + score). The mucin-like/PAT domain of Nfasc186 is predicted to be rich in O-linked glycosylation but this has been shown to be a minor contributor to the apparent molecular mass of Nfasc186 (Volkmer *et al*., 1992). Thus, the inclusion of an alternatively glycosylated 5th FNIII domain in Nfasc186 is a leading contender to partially account for the difference in apparent molecular mass between Nfasc186 and Nfasc155H, consistent with Koticha and colleagues (2005).

These ideas contribute to the evaluation of the potential differences between Nfasc155H and Nfasc155L. It has been proposed here that Nfasc155L is N-glycosylated at more sites than Nfasc155H in older animals and at even more sites in younger animals. The knowledge that the exons encoding the 5th FNIII domain are alternatively spliced and contain three possible sites for N-linked glycosylation immediately implicates it as a possible component of Nfasc155L that is lacking in Nfasc155H. While all of the other FNIII domains of L1 subfamily members are encoded by a pair of exons, the 5th FNIII domain of Nfasc has been observed in cDNAs as a half domain (Hassel *et al*., 1997), with the first exon being the more commonly expressed half and encoding two predicted sites of N-linked glycosylation. Additionally, Nfasc Ig-like domains are alternatively spliced much less frequently than are FNIII domains, with all six Ig-like domains being present in over half of the cDNA clones examined in the study of clones from embryonic days 6 and 16 by

Hassel and colleagues (1997).

While no definitive statements can be made, it is conceivable that Nfasc 155L contains the 5th FNIII domain and lacks the 3rd FNIII domain, which is also highly alternatively spliced (Hassel *et al.,* 1997) and contains only one predicted site of N-linked glycosylation (8/9 neural networks agree, + score; somewhat likely). This alternative exon usage may account for the differences in N-linked glycosylation observed between Nfasc155H and Nfasc155L, however exchange of the 3rd FNIII domain (12.3 kDa) for the 5th FNIII domain (10.2 kDa) only accounts 2.1 kDa. Since it has been shown here that Nfasc155H and Nfasc155L differ by 10 kDa after treatment with PNGase F, the remaining ~8 kDa could be accounted for by alternative usage of the highly alternatively spliced insert domains, calculated to be between 0.6 and 2.1 kDa each. Additional size variability may come from post-natal-specific alternative splicing of FNIII domains 1, 2, and 4 (10-12 kDa each) as well as each half domain of the 5th FNIII (4.6 and 5.7 kDa, respectively) that would not have been observed in the embryonic study of Hassel and colleagues (1997) and consistent with the initial expression of Nfasc155L between post-natal days 7 and 14.

Nfasc155H and Nfasc155L levels are altered in multiple sclerosis

The alterations regarding MS tissue indicate that while abundant Nfasc155L is not normally observed in human brain, it can become more prevalent in MS plaques. Concurrently, Nfasc155H appears to be lost in these same plaques insinuating that Nfasc155L forms from Nfasc155H under pathological mechanisms, but this does not

appear to be the case in either rats or mice. Resolution of this apparent conflict will require detailed studies with large sample sizes and immunohistochemical studies to define the disease status of each piece of tissue paired with western blots to distinguish Nfasc155H and Nfasc155L.

Two categories of possible scenarios exist; either rodents and humans follow the same mechanisms regarding expression and maintenance of Nfasc155H and Nfasc155L and ones where they differ. Considering that they are the same, rodents exhibit gradually increasing amounts Nfasc155L with age while Nfasc155H peaks near 30 days of age, drops sharply by 3 months, and is maintained until at least 5 months of age, such that Nfasc155L is the predominant form at 3 and 5 months of age. Predominant Nfasc155L is only observed in human tissue in the case of MS, however, Nfasc155L levels in human development have not been analyzed. Perhaps humans express barely detectable amounts Nfasc155L, but with the same function as rodent Nfasc155L, and the demyelination:remyelination occurrences of MS result in aberrant expression of myelin-related genes, resulting in elevated levels of Nfasc155L.

Considering that rodents and humans differ with regards to Nfasc155H and Nfasc155L, rodent and (likely) human Nfasc155H is a myelin paranode concentrated protein involved in cell adhesion. Rodent Nfasc155L appears to be involved in a process or processes that become more common in older animals. Unpublished observations from this laboratory have led to the supposition that rodent Nfasc155L could be involved in myelin compaction

via myelin:myelin adhesion, an idea consistent with observed ever-increasing numbers of paranodal loops, presumed to be additional wraps of myelin, as the animals age. Perhaps humans have another protein that fulfills this purpose, or the actual purpose of Nfasc155L, such that it is only expressed by humans as needed, and the demyelination:remyelination occurrences indicative of MS activate emergency myelin-related pathways involving Nfasc155L. Also, since rodent Nfasc155L has been shown to be differentially glycosylated with age, it is conceivable that human Nfasc155L is glycosylated such that it migrates along with Nfasc155H through life and that this glycosylation state is altered in MS, allowing for visualization of Nfasc155L. This idea is supported by the first sample in Figure 11B and by Figure 11C where the untreated samples contain one band and the PNGase F treated samples contain two bands (Nfasc155H and Nfasc155L).

Establishing the extended western blot protocol

Western blotting has become a technique so common that every lab has its own protocols and modifications. The technique used here to visualize the proteins of interest is one that has been optimized based on knowledge acquired while troubleshooting the original technique. While most protocols call for no particular percentage of gel, one hour of gel electrophoresis, and one hour of electrophoretic transfer, the protocol developed in this project uses 10% Ready Gels, three hours of gel electrophoresis, and two hours of electrophoretic transfer. The details of why this is the optimal protocol follows.

The proteins of interest in this project migrate slightly slower than the 150 kDa molecular weight standard (Kaleidoscope Ladder, Bio-Rad). As discussed earlier, Nfasc186 and Nfasc155 are recognized by the same pan-neurofascin antibodies and both proteins are seen on a western blot if these antibodies are applied. Separating these two protein bands from each other is a fairly simple task; however, caution must be taken to be sure that a gel is run long enough to allow for visualization of two distinct bands. In early efforts to do just this, it became clear that the band originally assigned as Nfasc155 migrates as two bands (Nfasc155H and Nfasc155L) when electrophoresis is extended beyond one hour. Attempts to study this novel finding led to gels being run for longer and longer times to allow the two new bands to be clearly distinguished from one another. Whereas one hour of electrophoresis revealed only Nfasc186 and Nfasc155, two hours of electrophoresis resulted in the Nfasc155 band dividing into two but the bands remained close enough to each other that they touched. Three hours of electrophoresis resolved this problem and made Nfasc186, Nfasc155H, and Nfasc155L clearly visible and distinct from one another. In the end, gels were run at 70 volts for 20-30 minutes to allow for protein stacking then at 150 volts until the 75 kDa ladder band reached the bottom of the gel (approximately another two and one half hours). This made for another problem, however, since most loading/transfer control proteins are below 50 kDa; ERK2 and β-actin migrate at approximately 42 kDa. To overcome this, a second western blot was performed on the day after the Nfasc one and run for only one hour after protein stacking with a one hour transfer.

At the same time, one hour of electrophoretic transfer at 100 Volts was observed to leave some of the high molecular weight Kaleidoscope ladder bands in the gel, demonstrating less than 100% efficiency in the transfer of large proteins. Proteins below 100 kDa were no longer visible in the gel after transfer while proteins 100 kDa and above were visible on the nitrocellulose membrane and in the gel. Increasing the transfer time from one hour to two hours and keeping the voltage at 100 resolved this problem (and showed more distinct Nfasc bands) but increased the amount of heat generated by the power supply. To overcome the heat of one hour of transfer, most protocols call for the transfer apparatus to be placed in a cooler that is then filled with ice water. Not mentioned in most protocols, but utilized in many laboratories, is the addition of an ice-filled chamber inside the transfer apparatus. Early troubles in perfecting this protocol came from not properly cooling the transfer apparatus during the one hour transfer. Upon realizing that a two hour transfer would be beneficial yet dangerously hot to the gel and/or membrane, transfers were carried out in a large plastic container (roughly five times the volume of the transfer apparatus) filled with ice water. This was sufficient to keep the transfer buffer, and presumably the gel sandwich, cold throughout the transfer. Refreshing the internal ice chamber after one hour of transfer aided in cooling.

Gradient gels work well for experiments involving two-three proteins when those proteins are notably different in size, 30 and 120 kDa for example. The higher concentration of acrylamide (the essence of the "gel") near the bottom of the gel prevents smaller proteins from exiting the gel. For visualization of only Nfasc186 and Nfasc155, almost any

percentage gel will work. As the novel banding pattern became more interesting, it was apparent that special considerations regarding the gel percentage would be needed. Gradient gels were utilized at this time in the laboratory but showed variable results. Early advice on how to optimally separate these two bands pointed toward 7.5% gels being ideal for the separation of larger proteins. While true, these gels are too weak to survive the harsh conditions that a gel will undergo during an extended run and a two hour transfer. The heat, pressure, and/or contact involved in blotting causes 7.5% gels to stick to the gel sandwich and become unusable. The next best attempt is 10% gels, which allowed for separation of all the proteins of interest and survive transfer.

Concluding Remarks

The developmentally variable presence of Nfasc155H and Nfasc155L may provide clues to some of the contradictory results presented in the literature (Charles *et al*., 2002; Bonnon *et al*., 2003; Gollan *et al*., 2003) regarding the requirements for contactin:Caspr:Nfasc155 interactions. It is conceivable that certain investigators were studying only Nfasc155H or only Nfasc155L while other investigators were studying both simultaneously but were unaware of this since Nfasc155H and Nfasc155L migrate together on gels when examining homogenates of younger animals. Additionally, the variable glycosylation presented here between Nfasc155H and Nfasc155L, as well as the variable glycosylation between young and old animal-derived Nfasc155L, may play a role in interactions with these proteins, comparable to those observed for contactin and Caspr (Gollan *et al*., 2003). Further understanding of the exact compositions of Nfasc155H and Nfasc155L will allow for

evaluative binding studies and will continue adding to the understanding of the formation and stability of the paranode and axon functional domains.

Literature Cited

Literature Cited

Albers, RW., Siegel GJ. 2006. Membrane Transport. In G. Siegel (ed.), Basic Neurochemistry: Molecular, Cellular, and Medical Aspects. Burlington, MA. Elsevier Academic Press. 73-94.

Alberts B., Johnson J., Lewis J., Raff M., Roberts K., Walter P. In B. Alberts, A. Johnson. J. Lewis, M. Raff, K. Roberts, P. Walter (ed.), Molecular Biology of the Cell. Oxford, UK. Garland Science. 617-650.

Aston-Jones G, Zhu Y, Card JP. 2004. Numerous GABAergic afferents to locus ceruleus in the pericerulear dendritic zone: Possible interneuronal pool. J Neurosci 24(9):2313-21.

Badlangana NL, Bhagwandin A, Fuxe K, Manger PR. 2007. Observations on the giraffe central nervous system related to the corticospinal tract, motor cortex and spinal cord: What difference does a long neck make? Neuroscience 148(2):522-34.

Barclay AN. 2003. Membrane proteins with immunoglobulin-like domains-a master superfamily of interaction molecules. Semin Immunol 15(4):215-23.

Basu S, Schultz AM, Basu M, Roseman S. 1971. Enzymatic synthesis of galactocerebroside by a galactosyltransferase from embryonic chicken brain. J Biol Chem 246(13):4272-9.

Bhat MA, Rios JC, Lu Y, Garcia-Fresco GP, Ching W, St Martin M, Li J, Einheber S, Chesler M, Rosenbluth J, Salzer JL, Bellen HJ. 2001. Axon-glia interactions and the domain organization of myelinated axons requires neurexin IV/Caspr/Paranodin. Neuron 30(2):369-83.

Black JA, Newcombe J, Trapp BD, Waxman SG. 2007. Sodium channel expression within chronic multiple sclerosis plaques. J Neuropathol Exp Neurol 66(9):828-37.

Boggs JM, Gao W, Hirahara Y. 2008. Myelin glycosphingolipids, galactosylceramide and sulfatide, participate in carbohydrate-carbohydrate interactions between apposed membranes and may form glycosynapses between oligodendrocyte and/or myelin membranes. Biochim Biophys Acta 1780(3):445-55.

Bonnon C, Goutebroze L, Denisenko-Nehrbass N, Girault JA, Faivre-Sarrailh C. 2003. The paranodal complex of F3/contactin and caspr/paranodin traffics to the cell surface via a non-conventional pathway. J Biol Chem 278(48):48339-47.

Bosio A, Binczek E, Stoffel W. 1996a. Molecular cloning and characterization of the mouse CGT gene encoding UDP-galactose ceramide-galactosyltransferase (cerebroside synthetase). Genomics 35(1):223-6.

Bosio A, Binczek E, Le Beau MM, Fernald AA, Stoffel W. 1996b. The human gene CGT encoding the UDP-galactose ceramide galactosyl transferase (cerebroside synthase): Cloning, characterization, and assignment to human chromosome 4, band q26. Genomics 34(1):69-75.

Bosio A, Binczek E, Stoffel W. 1996c. Functional breakdown of the lipid bilayer of the myelin membrane in central and peripheral nervous system by disrupted galactocerebroside synthesis. Proc Natl Acad Sci U S A 93(23):13280-5.

Boyle ME, Berglund EO, Murai KK, Weber L, Peles E, Ranscht B. 2001. Contactin orchestrates assembly of the septate-like junctions at the paranode in myelinated peripheral nerve. Neuron 30(2):385-97.

Braun L, Cannella D, Pinheiro AM, Kieffer S, Belrhali H, Garin J, Hakimi MA. 2008. The small ubiquitin-like modifier (SUMO)-conjugating system of *Toxoplasma gondii*. Int J Parasitol .

Buschard K, Josefsen K, Hansen SV, Horn T, Marshall MO, Persson H, Mansson JE, Fredman P. 1994. Sulphatide in islets of Langerhans and in organs affected in diabetic late complications: A study in human and animal tissue. Diabetologia 37(10):1000-6.

Charles P, Tait S, Faivre-Sarrailh C, Barbin G, Gunn-Moore F, Denisenko-Nehrbass N, Guennoc AM, Girault JA, Brophy PJ, Lubetzki C. 2002. Neurofascin is a glial receptor for the paranodin/Caspr-contactin axonal complex at the axoglial junction. Curr Biol 12(3):217-20.

Chernousov MA, Fogerty FJ, Koteliansky VE, Mosher DF. 1991. Role of the I-9 and III-1 modules of fibronectin in formation of an extracellular fibronectin matrix. J Biol Chem 266(17):10851-8.

Chiu SY. 1980. Asymmetry currents in the mammalian myelinated nerve. J Physiol 309:499-519.

Chiu SY and Schwarz W. 1987. Sodium and potassium currents in acutely demyelinated internodes of rabbit sciatic nerves. J Physiol 391:631-49.

Coetzee T, Dupree JL, Popko B. 1998. Demyelination and altered expression of myelin-associated glycoprotein isoforms in the central nervous system of galactolipid-deficient mice. J Neurosci Res 54(5):613-22.

Coetzee T, Li X, Fujita N, Marcus J, Suzuki K, Francke U, Popko B. 1996a. Molecular cloning, chromosomal mapping, and characterization of the mouse UDP-galactose:ceramide galactosyltransferase gene. Genomics 35(1):215-22.

Coetzee T, Fujita N, Dupree J, Shi R, Blight A, Suzuki K, Suzuki K, Popko B. 1996b. Myelination in the absence of galactocerebroside and sulfatide: Normal structure with abnormal function and regional instability. Cell 86(2):209-19.

Collinson JM, Marshall D, Gillespie CS, Brophy PJ. 1998. Transient expression of neurofascin by oligodendrocytes at the onset of myelinogenesis: Implications for mechanisms of axon-glial interaction. Glia 23(1):11-23.

Costantino-Ceccarini E and Morell P. 1973. Synthesis of galactosylceramide and glucosylceramide by mouse kidney preparations. J Biol Chem 248(23):8240-6.

Daniels MA, Hogquist KA, Jameson SC. 2002. Sweet 'n' sour: The impact of differential glycosylation on T cell responses. Nat Immunol 3(10):903-10.

Davis JQ and Bennett V. 1994. Ankyrin binding activity shared by the neurofascin/L1/NrCAM family of nervous system cell adhesion molecules. J Biol Chem 269(44):27163-6.

Davis JQ, Lambert S, Bennett V. 1996. Molecular composition of the node of Ranvier: Identification of ankyrin-binding cell adhesion molecules neurofascin (mucin+/third FNIII domain-) and NrCAM at nodal axon segments. J Cell Biol 135(5):1355-67.

Davis JQ, McLaughlin T, Bennett V. 1993. Ankyrin-binding proteins related to nervous system cell adhesion molecules: Candidates to provide transmembrane and intercellular connections in adult brain. J Cell Biol 121(1):121-33.

Dermietzel R. 1974. Junctions in the central nervous system of the cat. II. A contribution to the tertiary structure of the axonal-glial junctions in the paranodal region of the node of Ranvier. Cell Tissue Res 148(4):577-86.

Dietschy JM and Turley SD. 2004. Cholesterol metabolism in the central nervous system during early development and in the mature animal. J Lipid Res 45(8):1375-97.

Dupree JL, Girault JA, Popko B. 1999. Axo-glial interactions regulate the localization of axonal paranodal proteins. J Cell Biol 147(6):1145-52.

Dupree JL, Coetzee T, Blight A, Suzuki K, Popko B. 1998. Myelin galactolipids are essential for proper node of Ranvier formation in the CNS. J Neurosci 18(5):1642-9.

Einheber S, Zanazzi G, Ching W, Scherer S, Milner TA, Peles E, Salzer JL. 1997. The axonal membrane protein caspr, a homologue of neurexin IV, is a component of the septate-like paranodal junctions that assemble during myelination. J Cell Biol 139(6):1495-506.

Fernandez-Moran H.1950. Electron microscope examination of the myelin sheath and axial cylinder in the internodal section of neural fibers. Experientia 6(9):339-42.

Flores AI, Narayanan SP, Morse EN, Shick HE, Yin X, Kidd G, Avila RL, Kirschner DA, Macklin WB. 2008. Constitutively active Akt induces enhanced myelination in the CNS. J Neurosci 28(28):7174-83.

Foote SL, Bloom FE, Aston-Jones G. 1983. Nucleus locus ceruleus: New evidence of anatomical and physiological specificity. Physiol Rev 63(3):844-914.

Garver TD, Ren Q, Tuvia S, Bennett V. 1997. Tyrosine phosphorylation at a site highly conserved in the L1 family of cell adhesion molecules abolishes ankyrin binding and increases lateral mobility of neurofascin. J Cell Biol 137(3):703-14.

Gent WL, Gregson NA, Lovelidge CA, Winder AF. 1971. Protein content of myelin. Biochem J 122(5):49P-50P.

Gielen E, Baron W, Vandeven M, Steels P, Hoekstra D, Ameloot M. 2006. Rafts in oligodendrocytes: Evidence and structure-function relationship. Glia 54(6):499-512.

Gingras AC, Kennedy SG, O'Leary MA, Sonenberg N, Hay N. 1998. 4E-BP1, a repressor of mRNA translation, is phosphorylated and inactivated by the Akt(PKB) signaling pathway. Genes Dev 12(4):502-13.

Gollan L, Salomon D, Salzer JL, Peles E. 2003. Caspr regulates the processing of contactin and inhibits its binding to neurofascin. J Cell Biol 163(6):1213-8.

Greer JM and Lees MB. 2002. Myelin proteolipid protein-the first 50 years. Int J Biochem Cell Biol 34(3):211-5.

Grumet M. 1992. Structure, expression, and function of Ng-CAM, a member of the Immunoglobulin Superfamily involved in neuron-neuron and neuron-glia adhesion. J Neurosci Res 31(1):1-13.

Grumet M. 1991. Cell adhesion molecules and their subgroups in the nervous system. Curr Opin Neurobiol 1(3):370-6.

Han MH, Hwang SI, Roy DB, Lundgren DH, Price JV, Ousman SS, Fernald GH, Gerlitz B, Robinson WH, Baranzini SE, Grinnell BW, Raine CS, Sobel RA, Han DK, Steinman L. 2008. Proteomic analysis of active multiple sclerosis lesions reveals therapeutic targets. Nature 451(7182):1076-81.

Handa S, Yamato K, Ishizuka I, Suzuki A, Yamakawa T. 1974. Biosynthesis of seminolipid: Sulfation *in vivo* and *in vitro*. J Biochem 75(1):77-83.

Hartline DK and Colman DR. 2007. Rapid conduction and the evolution of giant axons and myelinated fibers. Curr Biol 17(1):R29-35.

Hassel B, Rathjen FG, Volkmer H. 1997. Organization of the neurofascin gene and analysis of developmentally regulated alternative splicing. J Biol Chem 272(45):28742-9.

Hille B., Catterall WA. 2006. Electrical Excitability and Ion Channels. In G. Siegel (ed.), Basic Neurochemistry: Molecular, Cellular, and Medical Aspects. Burlington, MA. Elsevier Academic Press. 95-109.

Hirano A and Dembitzer HM. 1967. A structural analysis of the myelin sheath in the central nervous system. J Cell Biol 34(2):555-67.

Hirano A., Llena JF. 1995. Morphology of central nervous axons. In S. Waxman, J. Kocsis, P. Stys (ed.), The Axon: Structure, Function and Pathophysiology. New York, NY: Oxford University Press. 49-67.

Hirano A, Sax DS, Zimmerman HM. 1969. The fine structure of the cerebella of a model of an inherited leukodystrophy in jimpy mice and their "normal" litter mates. Trans Am Neurol Assoc 94:174-7.

Hodgkin AL and Huxley AF. 1952. Currents carried by sodium and potassium ions through the membrane of the giant axon of *Loligo*. J Physiol 116(4):449-72.

Honke K, Hirahara Y, Dupree J, Suzuki K, Popko B, Fukushima K, Fukushima J, Nagasawa T, Yoshida N, Wada Y, Taniguchi N. 2002. Paranodal junction formation and spermatogenesis require sulfoglycolipids. Proc Natl Acad Sci U S A 99(7):4227-32.

Hooks SB and Cummings BS. 2008. Role of Ca^{2+}-independent phospholipase A(2) in cell growth and signaling. Biochem Pharmacol .

Howell OW, Palser A, Polito A, Melrose S, Zonta B, Scheiermann C, Vora AJ, Brophy PJ, Reynolds R. 2006. Disruption of neurofascin localization reveals early changes preceding demyelination and remyelination in multiple sclerosis. Brain 129(Pt 12):3173-85.

Hu Y, Doudevski I, Wood D, Moscarello M, Husted C, Genain C, Zasadzinski JA, Israelachvili J. 2004. Synergistic interactions of lipids and myelin basic protein. Proc Natl Acad Sci U S A 101(37):13466-71.

Ishizuka I. 1997. Chemistry and functional distribution of sulfoglycolipids. Prog Lipid Res 36(4):245-319.

Ivanov A and Aston-Jones G. 2001. Local opiate withdrawal in locus coeruleus neurons *in vitro*. J Neurophysiol 85(6):2388-97.

Ivanov A and Aston-Jones G. 1995. Extranuclear dendrites of locus coeruleus neurons: Activation by glutamate and modulation of activity by alpha adrenoceptors. J Neurophysiol 74(6):2427-36.

Jenkins SM, Kizhatil K, Kramarcy NR, Sen A, Sealock R, Bennett V. 2001. FIGQY phosphorylation defines discrete populations of L1 cell adhesion molecules at sites of cell-cell contact and in migrating neurons. J Cell Sci 114(Pt 21):3823-35.

Kenwrick S, Watkins A, De Angelis E. 2000. Neural cell recognition molecule L1: Relating biological complexity to human disease mutations. Hum Mol Genet 9(6):879-86.

Kirschner DA, Inouye H, Ganser AL, Mann V. 1989. Myelin membrane structure and composition correlated: A phylogenetic study. J Neurochem 53(5):1599-609.

Koticha D, Babiarz J, Kane-Goldsmith N, Jacob J, Raju K, Grumet M. 2005. Cell adhesion and neurite outgrowth are promoted by neurofascin NF155 and inhibited by NF186. Mol Cell Neurosci 30(1):137-48.

Laemmli UK. 1970. Cleavage of structural proteins during the assembly of the head of bacteriophage T4. Nature 227(5259):680-5.

Lee DP, Deonarine AS, Kienetz M, Zhu Q, Skrzypczak M, Chan M, Choy PC. 2001. A novel pathway for lipid biosynthesis: The direct acylation of glycerol. J Lipid Res 42(12):1979-86.

Leevers SJ, Weinkove D, MacDougall LK, Hafen E, Waterfield MD. 1996. The *Drosophila* phosphoinositide 3-kinase Dp110 promotes cell growth. EMBO J 15(23):6584-94.

Livingston RB, Pfenniger K, Moor H, Akert K. 1973. Specialized paranodal and interparanodal glial-axonal junctions in the peripheral and central nervous system: A freeze-etching study. Brain Res 58(1):1-24.

Marcus J, Dupree JL, Popko B. 2002. Myelin-associated glycoprotein and myelin galactolipids stabilize developing axo-glial interactions. J Cell Biol 156(3):567-77.

Marcus J, Honigbaum S, Shroff S, Honke K, Rosenbluth J, Dupree JL. 2006. Sulfatide is essential for the maintenance of CNS myelin and axon structure. Glia 53(4):372-81.

Menegoz M, Gaspar P, Le Bert M, Galvez T, Burgaya F, Palfrey C, Ezan P, Arnos F, Girault JA. 1997. Paranodin, a glycoprotein of neuronal paranodal membranes. Neuron 19(2):319-31.

Menon K, Rasband MN, Taylor CM, Brophy P, Bansal R, Pfeiffer SE. 2003. The myelin-axolemmal complex: Biochemical dissection and the role of galactosphingolipids. J Neurochem 87(4):995-1009.

Norgard KE, Moore KL, Diaz S, Stults NL, Ushiyama S, McEver RP, Cummings RD, Varki A. 1993. Characterization of a specific ligand for P-selectin on myeloid cells. A minor glycoprotein with sialylated O-linked oligosaccharides. J Biol Chem 268(17):12764-74.

Nussbaum JL, Bieth R, Mandel P. 1963. Phosphatides in myelin sheaths and repartition of sphingomyelin in the brain. Nature 198:586-7.

O'Brien JS. 1965. Stability of the myelin membrane. Science 147:1099-107.

Ogawa Y, Schafer DP, Horresh I, Bar V, Hales K, Yang Y, Susuki K, Peles E, Stankewich MC, Rasband MN. 2006. Spectrins and ankyrinB constitute a specialized paranodal cytoskeleton. J Neurosci 26(19):5230-9.

Peles E, Nativ M, Lustig M, Grumet M, Schilling J, Martinez R, Plowman GD, Schlessinger J. 1997. Identification of a novel contactin-associated transmembrane receptor with multiple domains implicated in protein-protein interactions. EMBO J 16(5):978-88.

Peters A., Palay S., Webster H. 1976. The Cellular Sheaths of Neurons. In A. Peters, S. Palay, H. Webster (ed.), The Fine Structure of the Nervous System. Philadelphia, PA: W.B. Saunders Company. 181-230.

Piccolino M. 2006. Luigi Galvani's path to animal electricity. C R Biol 329(5-6):303-18.

Poliak S and Peles E. 2003. The local differentiation of myelinated axons at nodes of Ranvier. Nat Rev Neurosci 4(12):968-80.

Poliak S, Salomon D, Elhanany H, Sabanay H, Kiernan B, Pevny L, Stewart CL, Xu X, Chiu SY, Shrager P, Furley AJ, Peles E. 2003. Juxtaparanodal clustering of shaker-like K+ channels in myelinated axons depends on Caspr2 and TAG-1. J Cell Biol 162(6):1149-60.

Pyne S, Lee SC, Long J, Pyne NJ. 2008. Role of sphingosine kinases and lipid phosphate phosphatases in regulating spatial sphingosine 1-phosphate signalling in health and disease. Cell Signal .

Quarles R., Macklin W., Morell P. 2006. Myelin Formation, Structure, and Biochemistry. In G. Siegel (ed.), Basic Neurochemistry: Molecular, Cellular, and Medical Aspects. Burlington, MA. Elsevier Academic Press. 51-71.

Ranscht B, Moss DJ, Thomas C. 1984. A neuronal surface glycoprotein associated with the cytoskeleton. J Cell Biol 99(5):1803-13.

Rasband MN. 2006. Neuron-glia interactions at the node of Ranvier. Results Probl Cell Differ 43:129-49.

Rasband MN. 2004. It's "juxta" potassium channel! J Neurosci Res 76(6):749-57.

Rathjen FG, Wolff JM, Chang S, Bonhoeffer F, Raper JA. 1987. Neurofascin: A novel chick cell-surface glycoprotein involved in neurite-neurite interactions. Cell 51(5):841-9.

Ren Q and Bennett V. 1998. Palmitoylation of neurofascin at a site in the membrane-spanning domain highly conserved among the L1 family of cell adhesion molecules. J Neurochem 70(5):1839-49.

Rios JC, Melendez-Vasquez CV, Einheber S, Lustig M, Grumet M, Hemperly J, Peles E, Salzer JL. 2000. Contactin-associated protein (caspr) and contactin form a complex that is targeted to the paranodal junctions during myelination. J Neurosci 20(22):8354-64.

Rosenbluth J. 1981. Freeze-fracture approaches to ionophore localization in normal and myelin-deficient nerves. Adv Neurol 31:391-418.

Rosenbluth J. 1976. Intramembranous particle distribution at the node of Ranvier and adjacent axolemma in myelinated axons of the frog brain. J Neurocytol 5(6):731-45.

Rosenbluth J. 1966. Redundant myelin sheaths and other ultrastructural features of the toad cerebellum. J Cell Biol 28(1):73-93.

Rosenbluth J, Dupree JL, Popko B. 2003. Nodal sodium channel domain integrity depends on the conformation of the paranodal junction, not on the presence of transverse bands. Glia 41(3):318-25.

Rosetti CM, Maggio B, Oliveira RG. 2008. The self-organization of lipids and proteins of myelin at the membrane interface. Molecular factors underlying the microheterogeneity of domain segregation. Biochim Biophys Acta 1778(7-8):1665-75.

Salzer JL. 1995. Mechanisms of adhesion between axons and glial cells. In S. Waxman, J. Kocsis, P. Stys (ed.), The Axon: Structure, Function and Pathophysiology. New York, NY: Oxford University Press. 164-194.

Schafer DP, Bansal R, Hedstrom KL, Pfeiffer SE, Rasband MN. 2004. Does paranode formation and maintenance require partitioning of neurofascin 155 into lipid rafts? J Neurosci 24(13):3176-85.

Shelke SV, Gao GP, Mesch S, Gathje H, Kelm S, Schwardt O, Ernst B. 2007. Synthesis of sialic acid derivatives as ligands for the myelin-associated glycoprotein (MAG). Bioorg Med Chem 15(14):4951-65.

Sherman DL, Tait S, Melrose S, Johnson R, Zonta B, Court FA, Macklin WB, Meek S, Smith AJ, Cottrell DF, Brophy PJ. 2005. Neurofascins are required to establish axonal domains for saltatory conduction. Neuron 48(5):737-42.

Simons M and Trotter J. 2007. Wrapping it up: The cell biology of myelination. Curr Opin Neurobiol 17(5):533-40.

Sims RJ,3rd and Reinberg D. 2008. Is there a code embedded in proteins that is based on post-translational modifications? Nat Rev Mol Cell Biol 9(10):815-20.

Stahl N, Jurevics H, Morell P, Suzuki K, Popko B. 1994. Isolation, characterization, and expression of cDNA clones that encode rat UDP-galactose:Ceramide galactosyltransferase. J Neurosci Res 38(2):234-42.

Sutherland DR, Abdullah KM, Cyopick P, Mellors A. 1992. Cleavage of the cell-surface O-sialoglycoproteins CD34, CD43, CD44, and CD45 by a novel glycoprotease from *Pasteurella haemolytica*. J Immunol 148(5):1458-64.

Tait S, Gunn-Moore F, Collinson JM, Huang J, Lubetzki C, Pedraza L, Sherman DL, Colman DR, Brophy PJ. 2000. An oligodendrocyte cell adhesion molecule at the site of assembly of the paranodal axo-glial junction. J Cell Biol 150(3):657-66.

Taylor C, Marta C, Bansal R, Pfeiffer S. 2004. The Transport, Assembly and Function of Myelin Lipids. In R.A. Lazzarini (ed.), Myelin biology and disorders. San Diego, CA: Elsevier Academic Press. 57-88.

Traka M, Dupree JL, Popko B, Karagogeos D. 2002. The neuronal adhesion protein TAG-1 is expressed by Schwann cells and oligodendrocytes and is localized to the juxtaparanodal region of myelinated fibers. J Neurosci 22(8):3016-24.

Traka M, Goutebroze L, Denisenko N, Bessa M, Nifli A, Havaki S, Iwakura Y, Fukamauchi F, Watanabe K, Soliven B, Girault JA, Karagogeous D. 2003. Association of TAG-1 with Caspr2 is essential for the molecular organization of juxtaparanodal regions of myelinated fibers. J Cell Biol 162(6):1161-72.

Trapp BD, Bo L, Mork S, Chang A. 1999. Pathogenesis of tissue injury in MS lesions. J Neuroimmunol 98(1):49-56.

Trapp BD, Andrews SB, Cootauco C, Quarles R. 1989. The myelin-associated glycoprotein is enriched in multivesicular bodies and periaxonal membranes of actively myelinating oligodendrocytes. J Cell Biol 109(5):2417-26.

Trapp BD, Bernier L, Andrews SB, Colman DR. 1988. Cellular and subcellular distribution of 2',3'-cyclic nucleotide 3'-phosphodiesterase and its mRNA in the rat central nervous system. J Neurochem 51(3):859-68.

Tuvia S, Garver TD, Bennett V. 1997. The phosphorylation state of the FIGQY tyrosine of neurofascin determines ankyrin-binding activity and patterns of cell segregation. Proc Natl Acad Sci U S A 94(24):12957-62.

Volkmer H, Zacharias U, Norenberg U, Rathjen FG. 1998. Dissection of complex molecular interactions of neurofascin with axonin-1, F11, and tenascin-R, which promote attachment and neurite formation of tectal cells. J Cell Biol 142(4):1083-93.

Volkmer H, Hassel B, Wolff JM, Frank R, Rathjen FG. 1992. Structure of the axonal surface recognition molecule neurofascin and its relationship to a neural subgroup of the Immunoglobulin Superfamily. J Cell Biol 118(1):149-61.

Watanabe I and Bingle GJ. 1972. Dysmyelination in "quaking" mouse. Electron microscopic study. J Neuropathol Exp Neurol 31(2):352-69.

Watanabe I, McCaman R, Dyken P, Zeman W. 1969. Absence of cerebral myelin sheaths in a case of presumed Pelizaeus-Merzbacher disease. Electron microscopic and biochemical studies. J Neuropathol Exp Neurol 28(2):243-56.

Waxman SG and Ritchie JM. 1985. Organization of ion channels in the myelinated nerve fiber. Science 228(4707):1502-7.

Wolswijk G and Balesar R. 2003. Changes in the expression and localization of the paranodal protein caspr on axons in chronic multiple sclerosis. Brain 126(Pt 7):1638-49.

Yahi N, Baghdiguian S, Moreau H, Fantini J. 1992. Galactosyl ceramide (or a closely related molecule) is the receptor for human immunodeficiency virus type 1 on human colon epithelial HT29 cells. J Virol 66(8):4848-54.

Yanagisawa K, Duncan ID, Hammang JP, Quarles RH. 1986. Myelin-deficient rat: Analysis of myelin proteins. J Neurochem 47(6):1901-7.

Zeis T, Graumann U, Reynolds R, Schaeren-Wiemers N. 2008. Normal-appearing white matter in multiple sclerosis is in a subtle balance between inflammation and neuroprotection. Brain 131(Pt 1):288-303.

Zhang Y, Li X, Becker KA, Gulbins E. 2008. Ceramide-enriched membrane domains-structure and function. Biochim Biophys Acta .

Zhao G and Hortsch M. 1998. The analysis of genomic structures in the L1 family of cell adhesion molecules provides no evidence for exon shuffling events after the separation of arthropod and chordate lineages. Gene 215(1):47-55.

Zoller I, Bussow H, Gieselmann V, Eckhardt M. 2005. Oligodendrocyte-specific ceramide galactosyltransferase (CGT) expression phenotypically rescues CGT-deficient mice and demonstrates that CGT activity does not limit brain galactosylceramide level. Glia 52(3):190-8.

Zonta B, Tait S, Melrose S, Anderson H, Harroch S, Higginson J, Sherman DL, Brophy PJ. 2008. Glial and neuronal isoforms of neurofascin have distinct roles in the assembly of nodes of Ranvier in the central nervous system. J Cell Biol 181(7):1169-77.

VITA

Anthony Dale Pomicter, known to all as Tony, came to Virginia Commonwealth University as an employee working under the title "Laboratory and Research Specialist" in August 2004. In January 2005, he enrolled in the neuroanatomy course as a non-degree seeking student and later became a part-time degree-seeking student in the Department of Anatomy and Neurobiology. Tony was the first student enrolled in both the Department of Anatomy and Neurobiology and the Molecular Biology and Genetics Program, consistent with his undergraduate degree focus of Development Biology and Genetics (Bachelor of Science: The Pennsylvania State University, 2002).

Previous research includes part-time undergraduate experience in an insect virology laboratory and full-time post-baccalaureate experience in a malaria genetics laboratory; both in the Department of Entomology at The Pennsylvania State University.

Tony was born in Plattsburgh, New York, U.S.A. on August 10, 1980 and has also lived in Alaska, Delaware, Pennsylvania, and Virginia; due to his father's career in the United States Air Force and his mother's Alaskan upbringing. He has one sister, born in 1984, who has been a dear friend since our childish fighting ending shortly after the family moved to Pennsylvania in 1994.